DISSERTATION IN PHYSICS

Charged Particles in Liquid He II

by Hidenobu HORI

THE OSAKA UNIVERSITY

GRADUATE SCHOOL OF SCIENCE

TOYONAKA, OSAKA

Contents

PART I

Thermal Properties of Hot Filament in Liquid Helium II

Abstract

Thermal properties of a hot tungsten filament and a gas sheath around the filament in liquid He II were investigated both experimentally and theoretically. It was found that the critical heat power W_c above which the gas sheath appears around the wire, can be explained by introducing an effective heat conductivity coming from the Khalatnikov theory. The stability of the gas sheath and its various properties were discussed by extending Knudsen's heat transport theory in gas and the treatment could well explain the experimental results. Frequently, the gas sheath makes an audible hiss and the phenomenon was analysed as an oscillation of the sheath.

§ 1. Introduction

The injection of excess charge carriers into liquid He II was initiated by Careri et al.[1] and also by Mayer and Reif[2] using the radioactive isotope $^{210}Po_{84}$ immersed in the liquid helium bath. α-particles emitting from the isotope produce both + and - ions in He II and almost all experiments have been done using this method. It is now well known that the negative charge carriers which are mainly electrons from so called bubble state while the positive ions such as He^+ make the iceberg or snowball state.[3] The effective mass was estimated to be about $100 \sim 200\ M_{He}$ for the bubble and about $50\ M_{He}$[4] for the latter where M_{He} means the atomic mass of helium.

On the other hand, there is an increasing requirment to have more dense charge carriers in the helium bath because the isotope method can only produce $10^5 \sim 10^7$ ions per c.c. so that it is not sufficient to do more extensive studies such as precise optic-alstudies or electron spin resonance. Therefore, various new methods to generate excess charge carriers in He II were tried by many researchers. As an example, we initiated the spark discharge method[5] to get more than 10^{10} charge carriers in the liquid. In 1968, Spangler and Hereford[6] obtained about 10^9/cc electrons by using a hot tungsten filament immersed in the liquid bath. This method is useful to study electron bubbles because it can only a lot of electrons. However, many phenomena associated with this method have not yet been analysed. In their experiment, tungsten filaments have been operated while

immersed in He II at temperatures up to 2500 K, and electron currents as high as 0.5 μA have been produced in the superfluid. The fluid in the vicinity of the filament remains quiescent under these conditions as a result of a stable vapor film or a gas sheath which forms around the filament. The process near the wire more nearly resembles film boiling when the helium depth is shallow ($\lesssim$ 3 cm) or temperature is high ($\gtrsim$ 1.8 K) while it seems to be a quiescent vapor bubble in the deep bath ($\gtrsim$ 10 cm) at low temperatures ($\lesssim$ 1.5 K). It is noted that these results are still qualitative and have no theoretical explanations.

On the other hand, our group tried to measure the size of the gas sheath[7] and obtained the following results: the diameter of the sheath is of the order of 100 μm and strongly depends on the liquid depth and temperatures of both the liquid and the filament. In their experiment, a tungsten filament of 4.5 μm in radius and 7 mm in length was placed in the microwave cavity where the electric field was maximum. A rectangular cavity of TE_{102} mode was used with a superconducting metal wall to get a high Q-value of about 10^4. When the gas sheath is produced in the cavity, a shift of the resonant frequency of the cavity occurs because the sheath removes the same volume of liquid out of the cavity. Thus we now have a systematic and quantitative datum about the size, and this allows us to extend the precise analysis of the gas sheath problem in liquid helium II, as will be shown in the present paper.

§ 2. Experimental

A commercially available tungsten wire with 9.1μm in diameter and~1 cm in length was used as the hot filament. The uniformity of the wire was checked by using a microscope. The wire showed the residual resistivity of $0.516 \pm 0.05 \times 10^{-6}$ Ω cm at liquid helium temperatures. As the electrical contact between the wire and copper leads is not always guaranteed because of the small diameter in the tungsten filament, the four terminal method was used for all electrical measurings as is usually done in semiconductor study.

A typical example of the IV-characteristic of the tungsten filament is shown in Fig. 1. At the low power region, the wire shows an ohmic current increase with residual resistivity. Above 0.07 Volts (point A), however, the ohmicity is broken showing a negative resistance and a large hysteresis between A and B. These curious phenomena may be due to the onset of a complex turbulent flow around the wire with an increase of the wire temperature. It is noticed that an audible hiss occurs at point B above which the gas sheath appears,[7] although the occurences of the hiss and gas sheath become not so clear when the liquid bath is shallow or the liquid temperature is high. Near point C, the filament begins to glimmer and the light becomes strong as the input power increases. The filament temperature was measured by using an optical pilometer and at the same time, the temperature was monitored by measuring the electrical resistivity of the filament. The results are shown

in Fig. 2. The hysteresis of the IV-characteristic is not shown in this figure. There is a considerable difference between the filament center and average temperatures showing the temperature gradient in the wire. When the filament temperature exceeds 1000 K, one can find the thermally emitted electrons in the liquid bath as was found by Spangler et. al.[6] A precise treatment of the electric properties of the system will be described elsewhere.

It should be noted that a reliable IV-characteristic was obtained only after the cleaning of the filament surface or after the heat flush of the wire. This means that one can not have a good datum when the filament is dirty. Therefore, the filament was heated up to 1500 K during several minutes before doing the experiment and almost of all surface impurities were eliminated by this procedure. As will be seen later, this fact is strongly concerned with the stability mechanism of the gas sheath.

§ 3. Critical Heat Flow and Heat Conductivity of He II

It is well known that the heat conductivity of superfluid He II is so large that the temperature gradient in the liquid is usually negligible. This is a reason why the boiling bubbles can not be seen in the He II. The presence of the gas sheath, however, means that the sheath is obviously a kind of bubble newly found in liquid He II giving rise a possibility that the

temperature gradient may be found near the filament when the heat flow is extremely strong. In such a case, a finite thermal conductivity coefficient is usually introduced by assuming a friction between two counterflow components of the super- and normal currents of the liquid based on the two fluid model. However, the practical friction data mainly obtained by the experiments of narrow channel liquid flow are scattered widely. Therefore, we tried to analyse our data by assuming a simple effective heat conductivity coefficient κ in the liquid and found that the experimental result can be explained by using the coefficient κ of Khalatnikov[8] and Zinoveva[9] determined dynamically from the damping of the second sound. The analysis was done in the following way. Let us first notice the presence of the critical heat flow W_c below which the wire shows an ohmic behavior keeping the wire temperature to be equal to that of the liquid. W_c estimated from Fig. 1 is 10 mW which corresponds to 5 Watt/cm^2. The critical heat flow means that the surface temperature of the filament can be kept to the liquid temperature till the heat flow increases up to W_c. The situation can be explained by Fig. 3. Under an equilibrium condition usually realized in experiments, the liquid surface is at point S. This means that the vapor pressure P_1 under the temperature T_1 should be on the phase boundary. When the filament is placed h cm below the surface, the liquid near the wire should be on A because of the additive pressure coming from the liquid above the wire. The pressure difference $P_o - P_1$ is of course $g\rho h$ where g is the gravitational constant and ρ is the liquid helium density.

As the heat flow increases, the liquid temperature on the wire surface increases but it does not beyond T_o because the gas sheath will appear above T_o. Therefore, it is easily expected that W_c depends on both the depth and temperature of the liquid.

We consider the two dimensional heat flow. Then the temperature gradient dT/dr is written by

$$\kappa(dT/dr) = - Q/2\pi r, \qquad (1)$$

where Q means the total heat flow per unit length of the wire. As is shown in Fig. 4, we assume that the tungsten wire with radius r_o is at the temperature T_o and any temperature gradient exists beyond r_1 in the liquid. Many years ago, Khalatnikov[8] calculated the temperature dependence of the thermal conductivity and it showed a good agreement with the experimental results determined from the attenuation of the second sound experiment, as is given in Fig. 5. For simplicity, it is assumed that the thermal conductivity in our experiment is expressed by the straight line in Fig. 5. This means that κ is written as

$$\kappa = 0.65 \exp(-4.6T), \qquad (2)$$

with the unit of Watt, sec^{-1}, cm^{-1}, $deg.^{-1}$ Using eq.(2) in eq.(1), the following relation is obtained:

$$\exp(-4.6T_1) - \exp(-4.6T_o) = 2.6Q \log_{10}(r_1/r_o). \qquad (3)$$

Accordingly, the critical heat power can be written as

$$W_c = (1/2\pi r_o)\{\exp(-4.6T_1) - \exp(-4.6T_o)\}/2.6\log_{10}(r_1/r_o). \quad (4)$$

The liquid temperature T_1 was measured by both the carbon resistor and the vapor pressure. To determine T_o, we write the pressure P_o at the wire as

$$P_o = P_s + g\rho h, \quad (5)$$

where P_s represents the vapor pressure at the liquid surface. Then $T_o(P_o)$ can be numerically obtained from the well known vapor pressure diagram of the liquid helium. We measured the critical heat power W_c as a function the helium liquid depth h as is shown in Fig. 6, where the data obtained by Vinson et al.[10] are also shown. The theoretical curve is drawn by assuming,

$$\log_{10}(r_1/r_o) = 0.054, \quad r_1/r_o = 1.13, \quad (6)$$

The theoretical curve in Fig. 6 well explained the experimental results. It is interesting to note that the region where the liquid has the temperature gradient is limited in a very small region and its thickness is estimated to be about 0.5 μm. The result seems to be appropriate because the liquid helium II is substantially a super fluid having an extremely good thermal conductivity.

Concerning with the results given in Fig. 6, the following points should be considered. Firstly, the experimental condition to keep a rigid two dimensionality is usually difficult to obtain. This is because the long uniform wire condition was hard to get. Accordingly, three dimensional heat leak was inevitable. Considering this fact, $r_1 - r_o$ may be between 0.5 and 1.0 μm. Secondary, a deviation between the theory and experiment becomes large when the helium bath level is shallow. Concerning with this point, it is noted that the gas sheath above W_c is unstable in the shallow region. Finally, eq.(4) can not explain the high temperature data near T_λ. Two possibilities may be considered. One of them is the effect of instability of the gas sheath at high temperatures and the other may be due to the fact that the temperature dependence of the thermal conductivity could not be explained by eq.(2). We also tried to use the extensive line of the Khalatnikov theory but a good agreement with the experimental results was not obtained.

§ 4. Stability of Gas Sheath

As is described before, the gas sheath is clearly observed around the filament when the input power exceeds the critical power W_c. However, it is not so stable between points B and C of Fig. 1 and it becomes also unstable when the liquid depth is shallow or the liquid temperature is high.[10 12)] The measured gas sheath radius is shown in Fig. 7 as a function of the filament temperature.[7)] It is assumed that the sheath radius R is

much larger than the filament radius r_o. As is seen in Fig. 7, this assumption is appropriate except the low temperature region where the sheath itself does not have a clear form. Now the mechanical and thermal stabilities of the gas sheath are considered in the following way: helium gas atoms in the sheath transport the energy W from the wire surface to the liquid surface with accomodation coefficients β and α , respectively. The gas pressure P would be calculated by summing up the momentum change of gas molecules at the liquid wall so as to balance to the sum of the residual gas pressure in the cryostat and the liquid pressure at the filament position.* It is noticed that the usual heat transport theory developed by Knudsen[13] can not be applicable because the sheath radius R is temperature and pressure dependent. Accordingly, the Knudsen theory should be modified. The accomodation coefficient, β is defined as usual by

$$\beta = (T_r - T_i)/(T_w - T_i), \qquad T_i \ll T_w, T_r, \qquad (7)$$

where T_r is the effective temperature of the reflected molecules from the wire, T_w is the wire temperature, and T_i is the initial temperature of molecules before collision. α is defined similarly. We consider a successive collision cycle given in Fig. 8. At a time t_o, a molecule collides to the wire and gets an energy βE_w, where E_w means the molecule energy corresponding to T_w. Then the molecule flies toward the liquid wall with velocity in the radial plane of the sheath as $(4\beta E_w/3M_{He})^{1/2}$. At $t = t_1$, the

---

* We can consider the mean free path of He atom in the sheath long, in fact, 0.1 mm or more under this experimental conditions.

molecule collides to the liquid wall with an energy loss $E_s\alpha$, and a momentum change $(4M_{He}/3)^{1/2}\{(\beta E_w)^{1/2} + (\varepsilon E_s + E_l)^{1/2}\}$, where E_l is the molecular energy corresponding to the liquid wall temperature and E_s is given as $\beta E_w - E_l$. ε means $1 - \alpha$. The flight time $t_l - t_o$ is given as $R(3M_{He}/4\beta E_w)^{1/2}$. For collisions from t_l to t_o to the liquid wall, it is assumed that the molecule flies a mean distance L between t_j and t_{j+1}. L is simply calculated as $4R/\pi$. The kinetic energy of the molecule after the m-th collision becomes $E_s\varepsilon^m + E_l$ and after that the molecule goes to the next cylle followed by the filament collision at t_{m+1}. Comparing the surface areas of the filament and liquid, m is given by R/r_o. Thus, the energy transfer, resultant momentum change and total time for one cycle can be calculated. We consider such molecules of number n/cc and calculate the energy transfer W per unit time and the pressure at the wire. Neglecting higher order terms, the results are given as follows:

$$P = (\pi n E_s/6)\left\{1 + 2\sum_{n=1}^{m-1}(\varepsilon^n + E_l/E_s)^{1/2}\right\} \times \left\{1 + (4/\pi)\sum_{n=1}^{m-1}(\varepsilon^n + E_l/E_s)^{-1/2}\right\}^{-1} \quad (8)$$

$$W = (3\pi RP/2)(4\beta E_w/3M_{He})^{1/2}\left\{1 + 2\sum_{n=1}^{m-1}(\varepsilon^n + E_l/E_s)^{1/2}\right\}^{-1}, \quad (9)$$

where P in eq.(9) is equal to eq.(8) and it is easily obtained from the experiment. Eq.(8) is valuable for estimation of n, namely, the gas density in the sheath.

In our model, the pressure is assumed to be uniform in the sheath. This assumption may be satisfied when the radius R is not so large. The sum in eq.(9) was obtained by replacing it as an integral form, being m to be much larger than unity. Then the energy flow W is written as

$$W = \frac{3\pi}{\sqrt{2}} PR(k\beta T_w/M_{He})^{1/2} / \left\{ 1 + 2m(T_1/\beta T_w)^{1/2} + 4/\alpha(1 + \alpha/2) \right\}, \quad (10)$$

where k is the Boltzmann constant and T_1 is the liquid helium temperature. Using experimental values of P, R, T_1, and T_w with the observed thermal loss W, the best values of α and β were determined as

$$\alpha = 0.27, \qquad \beta = 0.10. \quad (11)$$

The comparison with the theory and experiment is shown in Fig. 9. For the evaluation of the heat flow in the liquid, the light energy emitted from the wire is reduced from the total energy given to the wire.[6] It is noticed that the value of β between tungsten filament and helium gas is $0.05 \sim 0.5$[14] depending on the surface condition. The value of course becomes small when the surface is clean and it is also seen in our experiment. The fact that α is larger than β seems to be reasonable because He atom may be more inelastic at the liquid wall. When R becomes large, our model may be not so well because of the temperature gradient in the sheath and this may be a reason why the deviation in Fig. 9 becomes large at the high filament temperature regions.

§ 5. Oscillation of Gas Sheath

The frequency spectrum of the audible hiss or sound was analysed experimentally and the main frequency was estimated to be 1~2 kHz. The origin of this oscillation is considered as follows: first, it is easily shown that the sound comes from neither surface wave nor compressive wave of the sheath. Equation of motion of these waves can be calculated by solving the two dimensional wave equation and it is reduced to a well known Bessel function. Under the present experimental condition, however, the surface wave frequency is about 10 Mc and the compressive frequency is about 500 kc so that these frequencies are so far from the experimental data. The filament oscillation was also tested but it was of the order of 10 cycles.[7)]

The most plausible origin of the sound was attributed to the translational vibration of the sheath around the wire without changing its size and shape. This means that a restoring force due to an unbalanced gas pressure in the sheath occurs when the center of the sheath deviates from the regular position. As it is difficult to solve such a problem strictly, we tried to calculate the frequency as follows: the effective mass of the sheath should be of the order of liquid mass with the same volume as is usually done in hydrodynamics.[15)] The restoring force is evaluated by comparing the pressure difference produced by local heating and cooling due to the deviation of the sheath center. The result shows that the frequency is of the order of 0.5~5 kc if the adiavatic condition is assumed in the sheath. Thus, the result seems to be in good agreement with experiment.

References

1) G. Careri, J. Reuss, F. Scaramuzzi and J.O. Thomson: Proc. LT-5 (Wisconsin) (1957) 79, Nuovo Cimento (B) 13 (1959) 186.

2) L. Meyer and F. Reif: Phys. Rev. 110 (1958) 279, Phys. Rev. Letters 5 (1960) 1, Phys. Rev. 119 (1960) 1164.

3) K.R. Atkins: Phys. Rev. 116 (1959) 1339.

4) A.J. Dahm and T.M. Sanders,Jr.:Phys. Rev. Letters 17(1966)126.

5) M. Date, H. Hori, and H. Kamata: Proc. LT-12 (Kyoto)(1970)93.

6) G.E. Spangler and F.L. Hereford:Phys. Rev. Letters 20(1968)1229.

7) K. Okuda, Y. Inaba and M. Date: to be published in J. Phys. Soc. Japan.

8) I.M. Khalatnikov: J. Exp. Theor. Phys. USSR 23 (1952) 21.

9) K.N. Zinoveva: J. Exp. Theor. Phys. USSR 31 (1956) 31.

10) J.S. Vinson, F.J. Agee, R.J. Manning and F.L. Hereford: Phys. Rev. 168 (1968) 180.

11) F.E. Moss, F.L. Hereford, F.J. Agee and J.S. Vinson: Phys. Rev. Letters 14 (1965) 813.

12) D.M. Sitton and F.E. Moss: Phys. Rev. Letters 23 (1969) 1090.

13) M. Knudsen: Ann. der Phys. 31 (1910) 205.

14) H. Kumagai and G. Honjo: Vaccum Physics and its Applications, (in Japanese) Shokabo (1970) 70.

15) H. Lamb: Hydrodynamics, Cambridge Univ. Press, (1932).

Figure Captions

Fig. 1. IV-characteristic of a tungsten filament. Dotted limes show the hysteresis effect. An average power is also shown.

Fig. 2. IV-characteristic and the filament temperature. The temperature of the wire center was measured by a pilometer while the mean temperature was estimated from the resistivity.

Fig. 3. Pressure and temperature phase diagram (not in scale).

Fig. 4. Cut view of the wire and the surrounding liquid He II. The temperature of the wire with the radius r_o is T_o. There is a temperature gradient between r_o and r_1 but no temperature gradient is assumed out of r_1.

Fig. 5. Thermal conductivity coefficient κ of liquid He II. The curved line was given by Khalatnikov and open circles were obtained by Zinoveva experimentally. A straight line shows the present approximation given in the text.

Fig. 6. Critical heat power W_c as a function of liquid depth.

Fig. 7. Gas sheath radius as a function of filament temperature.

Fig. 8. Collision times in a cycle. At t_o and t_{m+1}, the gas molecule collides to the wire surface and other times show the collision to the liquid helium wall.

Fig. 9. Heat flow per unit length of the wire as a function of filament temperature. The theoretical curve is drawn by eq.(12) with $\alpha = 0.27$ and $\beta = 0.10$.

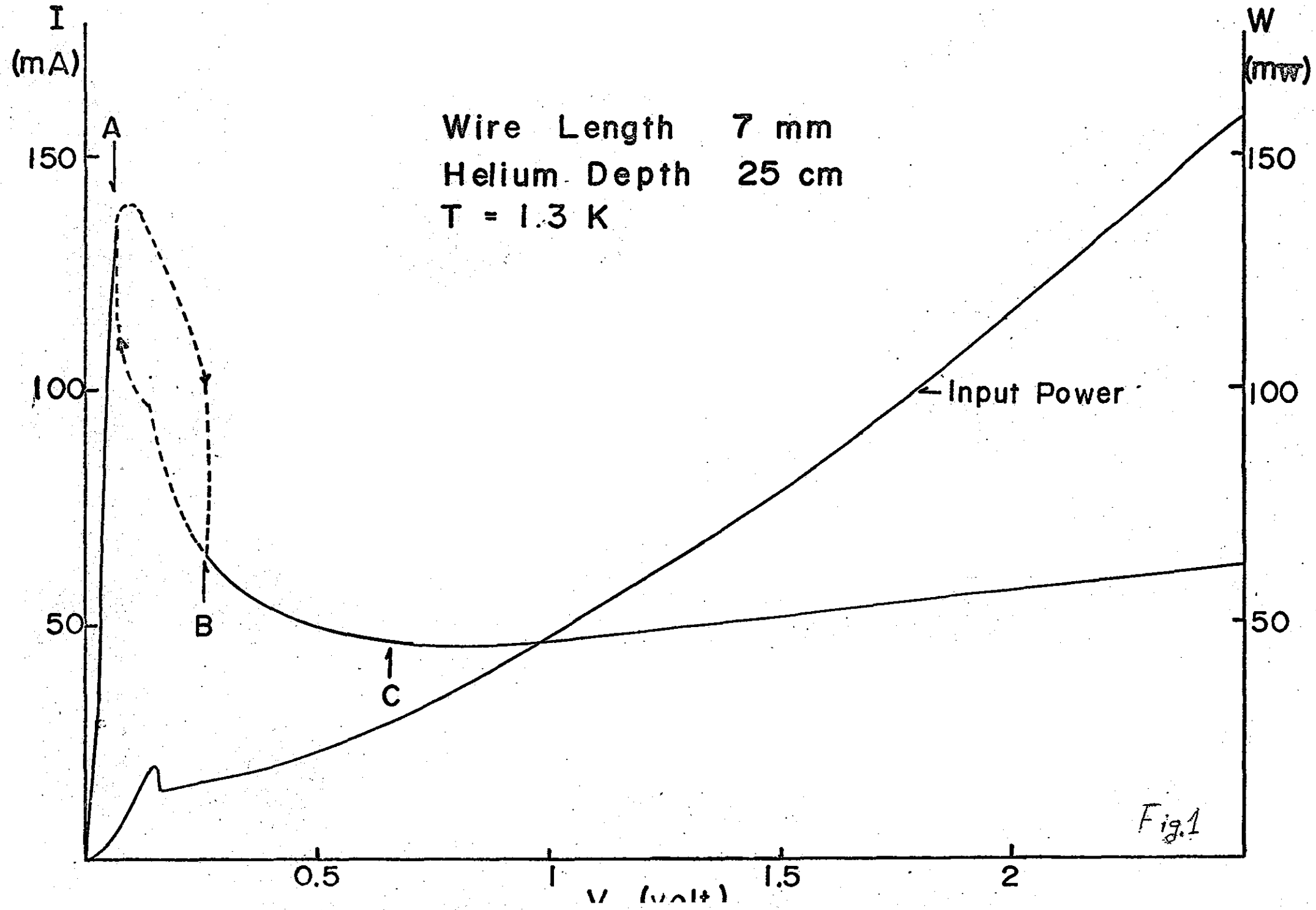
I
(mA)
W
(mW)
Wire Length 7 mm
Helium Depth 25 cm
T = 1.3 K
A
B
C
150
100
50
Input Power
0.5
1
1.5
2
V (volt)
Fig.1

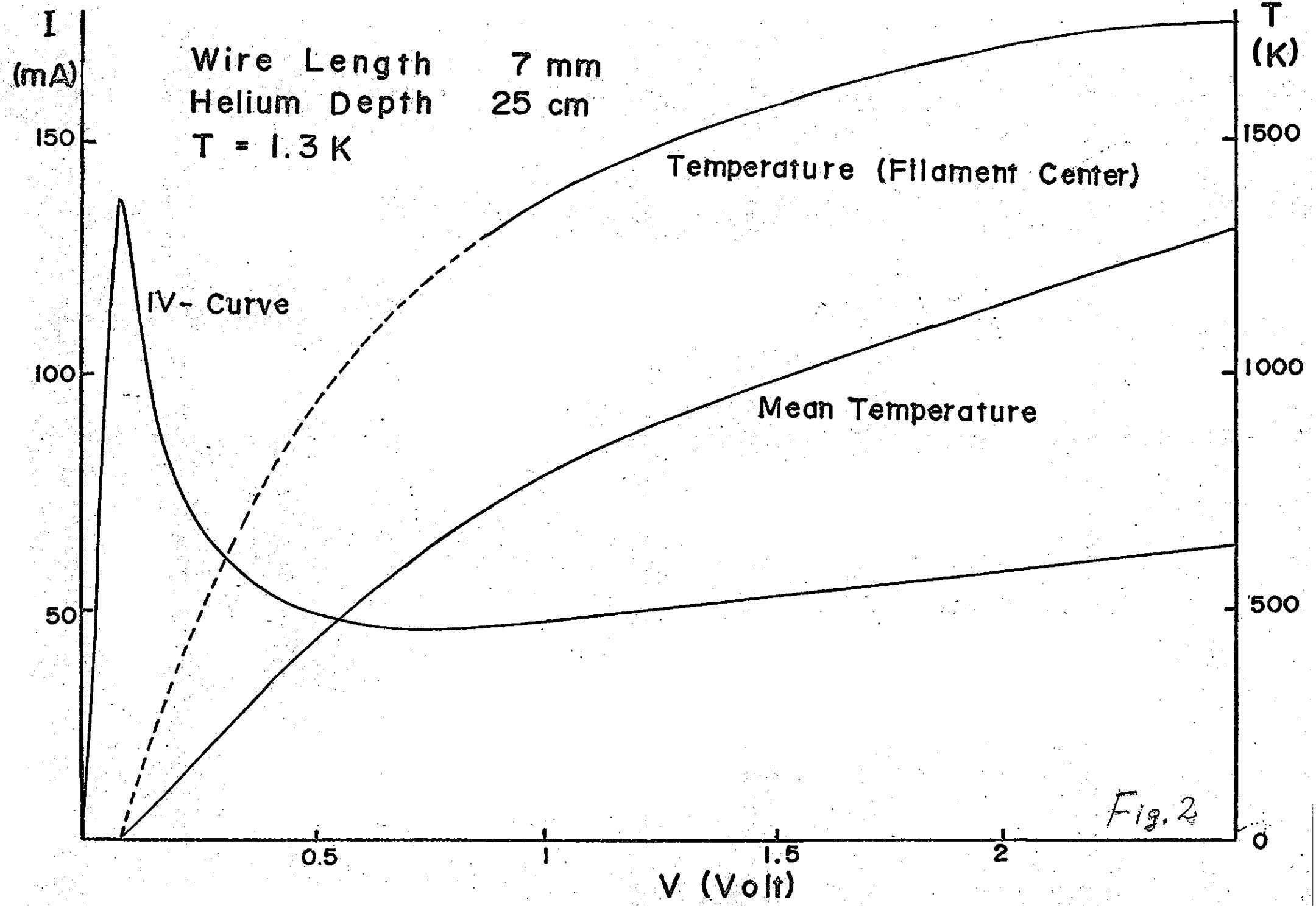
I
(mA)
Wire Length 7 mm
Helium Depth 25 cm
T = 1.3 K
150
100
50
IV- Curve
Temperature (Filament Center)
Mean Temperature
T
(K)
1500
1000
500
0
0.5
1
1.5
2
V (Volt)

Fig. 2

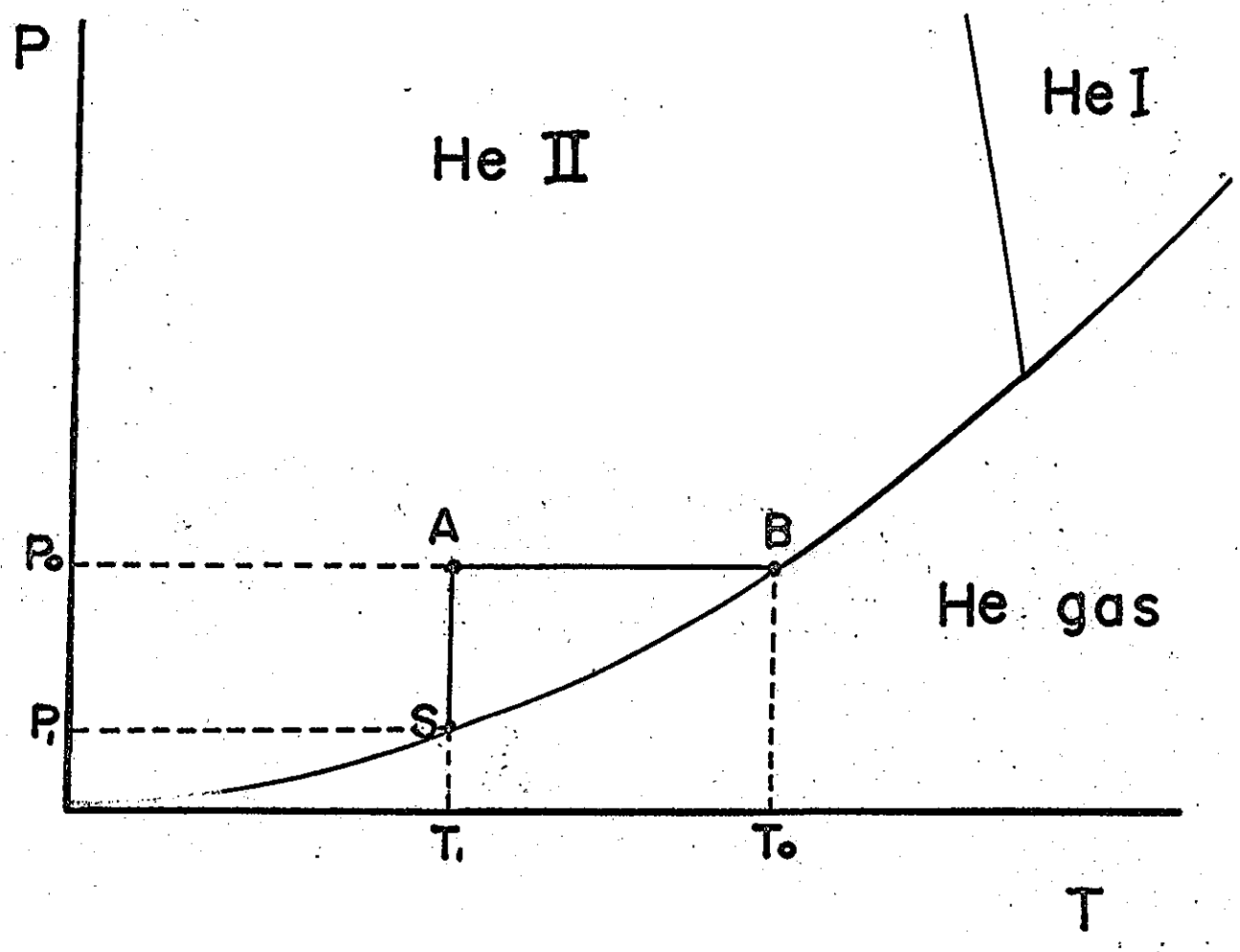

Fig. 3

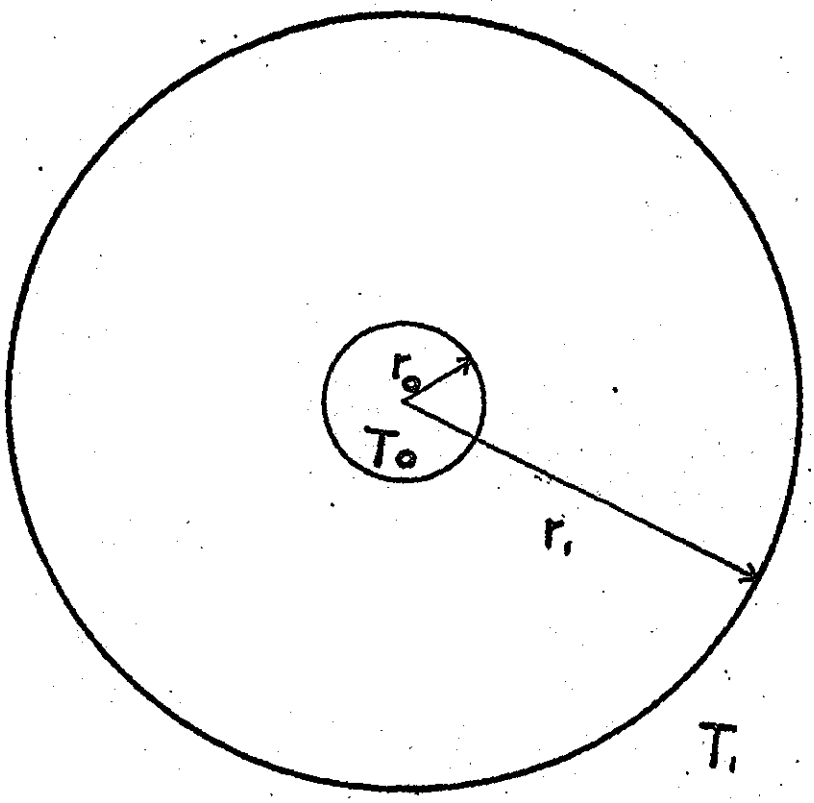

$T_o > T_1$

Fig. 4

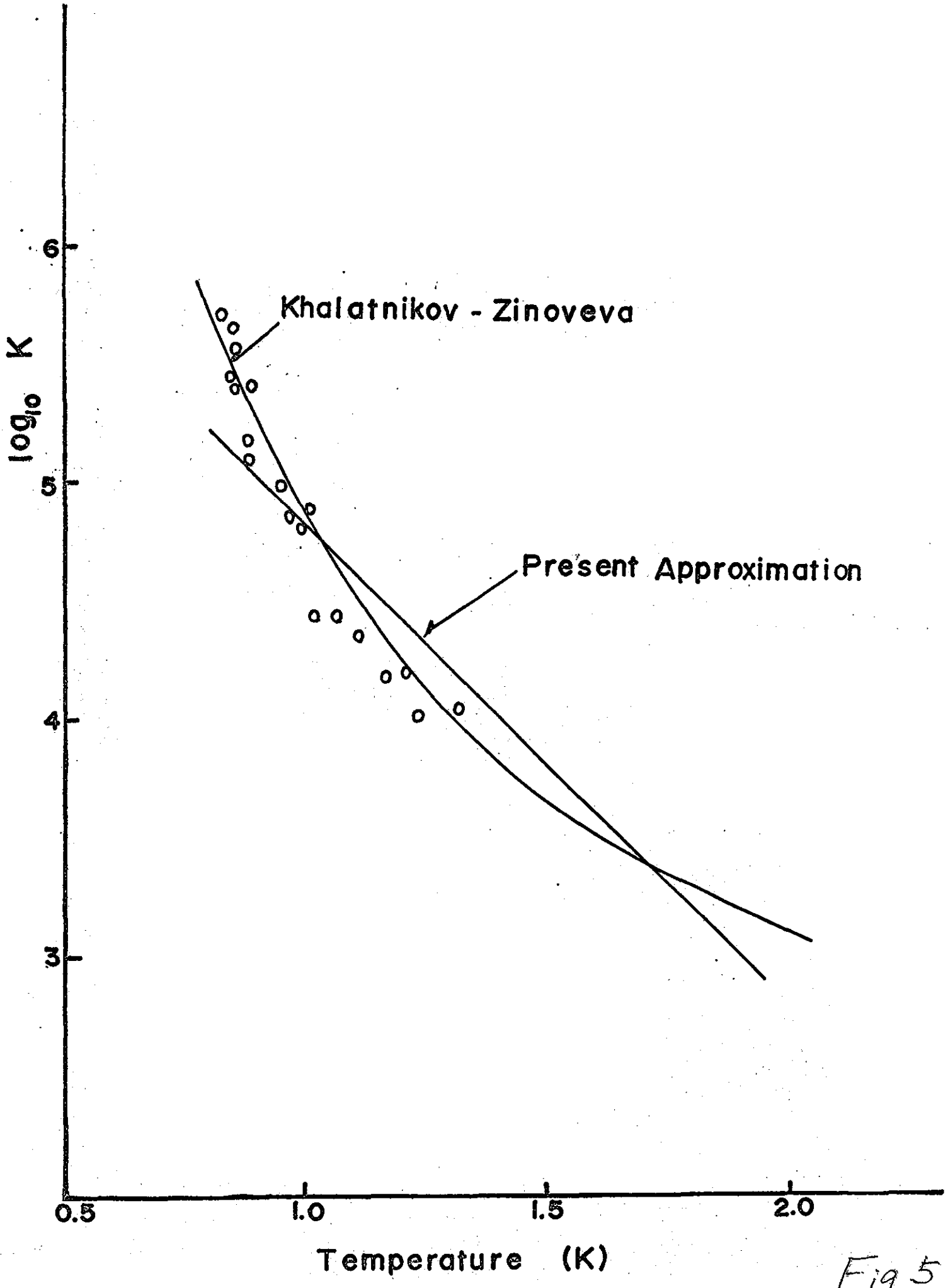
Khalatnikov - Zinoveva
Present Approximation
$\log_{10} K$
6
5
4
3
0.5
1.0
1.5
2.0
Temperature (K)

Fig. 5

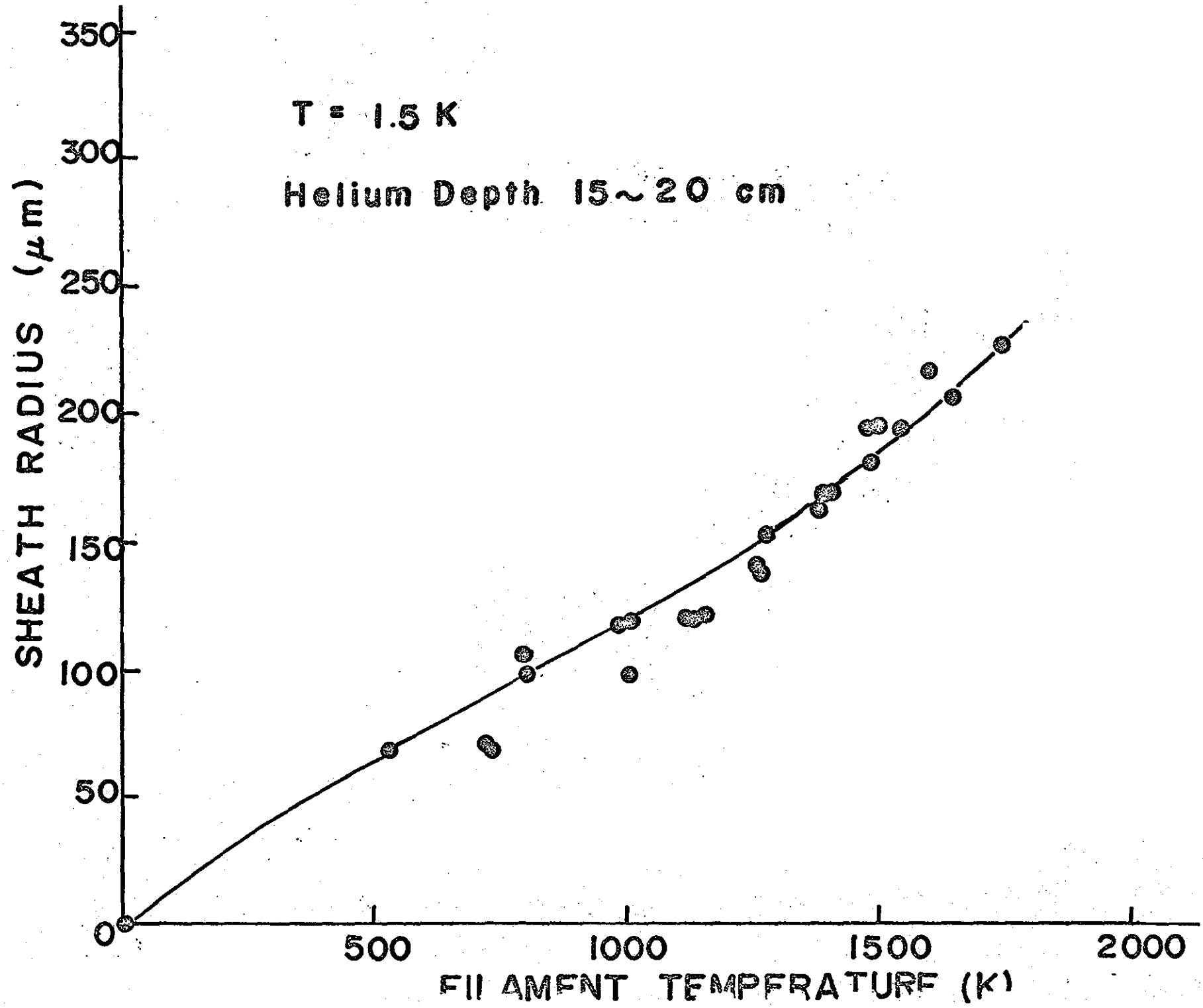
T = 1.5 K
Helium Depth 15~20 cm
SHEATH RADIUS (μm)
350
300
250
200
150
100
50
0
500
1000
1500
2000
FILAMENT TEMPERATURE (K)

Fig. 6

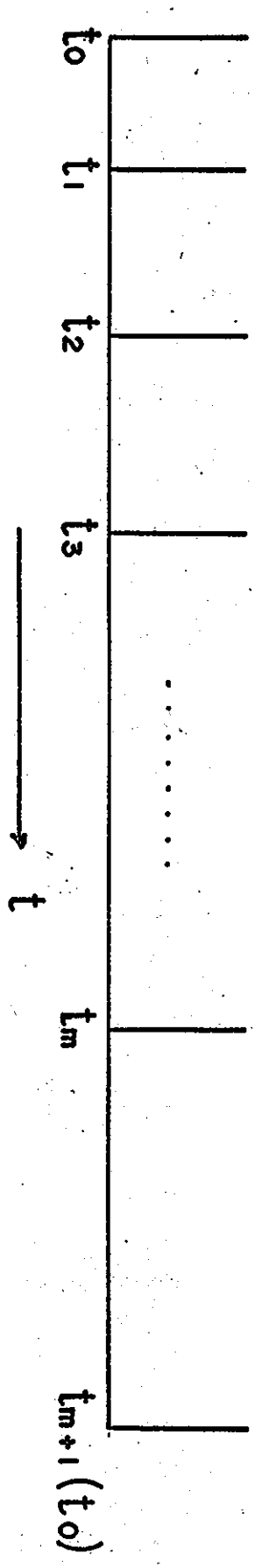

Fig. 7

Fig. 8

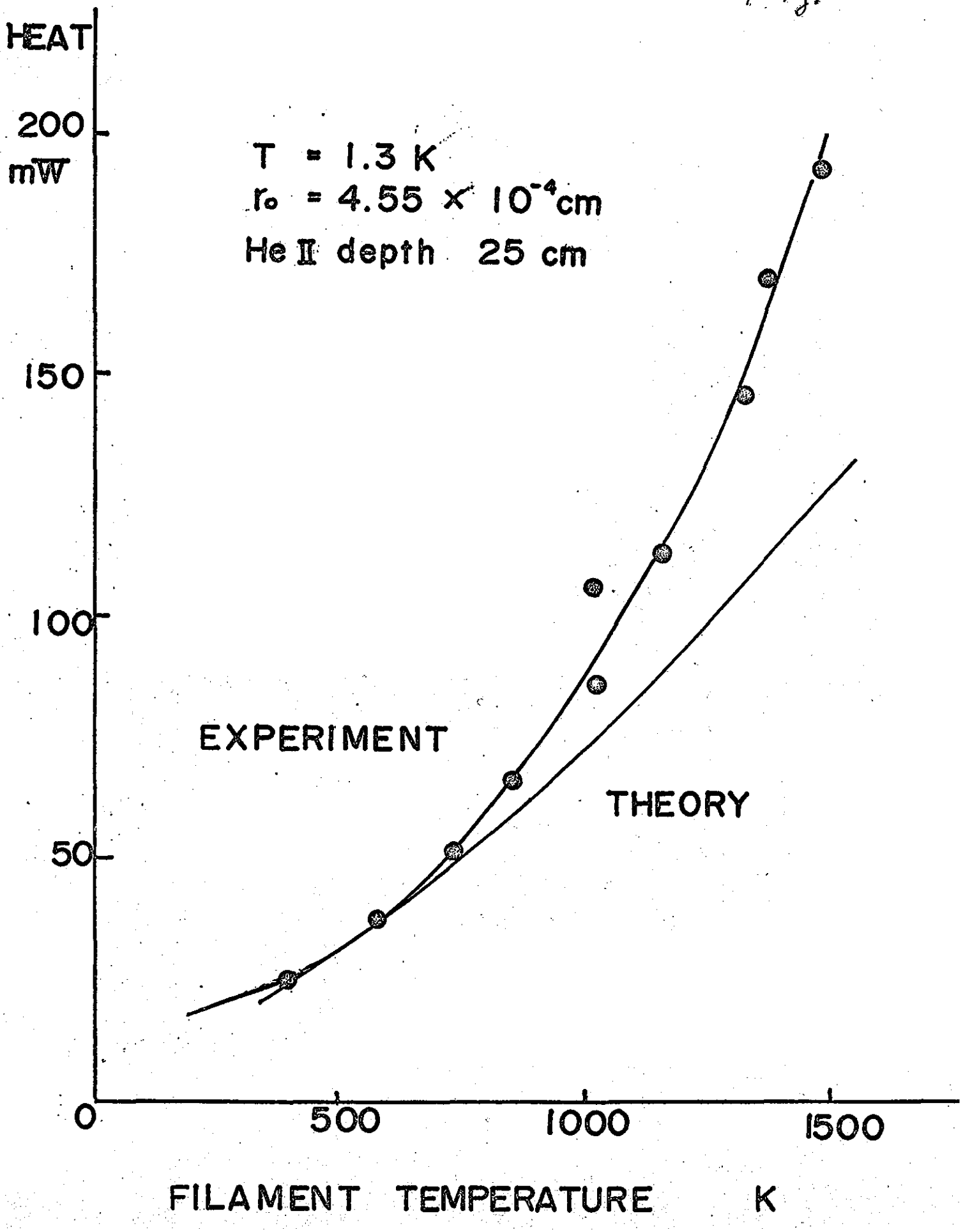
HEAT
200
mW
150
100
50
0
T = 1.3 K
r_o = 4.55 × 10^{-4} cm
He II depth 25 cm
EXPERIMENT
THEORY
500
1000
1500
FILAMENT TEMPERATURE K

PART II

Electrical Properties of Electron bubble in Liquid Helium II

Abstract

Electrical properties of electron bubble produced by a hot tungsten filament immersed in the liquid helium bath were investigated. The electrical current between the filament and the surrounding plate could well be explained by an ohmic flow of the bubble under a strong space charge field. The mobility of the electron bubble was strongly field dependent and the roton creation process was newly introduced for the bubble motion in addition to the well known processes of the phonon and roton scatterings and the interaction between vortex and ion.

§ 1. Introduction

Since the mobilities of charged particles in superfluid helium II were measured by Careri et al.[1] and Meyer and Reif,[2] various properties of charged impurities in the liquid bath have been investigated by many reseachers. The main technique for generating charged particles in liquid helium was the isotope method. α-particles emitted from the polonium isotope immersed in the liquid helium bath produce both + and - ions with the charge intensity of about $10^5 \sim 10^7$/cc. On the other hand, several methods for generation of more dense charge carriers in He II were tried by other groups. Of these new techniques, the hot filament method initiated by Spangler and Hereford[3] seems to be useful for the electron bubble study because it supplies only the electron bubble and no other + or - charged particles. They operated tungsten filaments of 3 and 5 μ diameter in liquid He II at temperatures up to 2500 K and have measured electron bubble currents as high as 0.5 μA injected into the He II bath. As a result of a stable vapor film or sheath which forms around a heated filament, it is thermally insulated to a high degree from the bath. To investigate the thermal electrons emitted from the filament, they made a diode consisted of a straight 1.5 cm length of tungsten wire surrounded by a 2 cm diameter gold plated cylindrical brass anode. They found the IV-characteristic of the diode at 1.3 K as is shown in Fig. 1. It was pointed out that the sheath is a surprisingly good thermal insulator. In the case

of a 3 μm diameter filament, for example, a temperature of 1650 K was obtained in vacuum at a filament power of 117 mW. When it was immersed in He II at a depth of 5 cm, 168 mW was required to obtain the same temperature. Hence, the He II bath was dissipatiog only 51 mW or approximately 30 % of the total filament power, the remainder being radiated. Such a surprising heat insulation was recently analysed by our group.[4] In this paper, the electronic properties of the diode are analysed. As will be seen in the following sections, the curious IV-characteristics obtained by Spangler et al. can be understood by assuming a strong space charge field in the diode.

§ 2. IV-Characteristic under a Space Charge Field

It is convenient to derive a general formula for explaining the relation between the current I and the voltage V before going to discuss the experimental results. Consider a two dimentional diode consisted of a filament with radius r_o and an anode or plate with radius r_2 as is shown in Fig. 2. r_1 is the gas sheath radius which is usually of the order of 100 μm.[5] The anode radius r_2 was changed between 0.1 and 1 cm.

As the filament temperature increases, the emission current i_o of thermal electrons with mass m and charge e increases according to the well known Richardson formula,

$$i_o = (4\pi emk^2T^2/h^3)\exp(-\phi/kT),$$

where ϕ is the work function of tungsten metal and was determined by Nichols[6] as 4.5 eV. The total current of thermal electrons from the filament per unit length can be calculated by using eq.(1) and the result shows that it is about 1 mA (10^3 μA) when the filament temperature is 2500 K. On the other hand, the observed current in the liquid was less than 1 μA. Hence it is strongly suggested that the current is suppressed by space charged around the wire.

The electric field E under a space charge density ρ can be obtained by solving

$$\text{div } E = 4\pi\rho/\varepsilon, \qquad (1)$$

where ε represents the dielectric constant which is assumed to be unity. Eq.(1) is solved without ϕ and z dependences in the cylindrical coordinates and the equation is written by

$$dE(r)/dr + E(r)/r = 4\pi\rho(r) = 4\pi en(r), \qquad (2)$$

where e is the electron charge and n is the electron density /cc. The total current I under a drift velocity v(r) is written as

$$I = 2\pi r\rho(r)v(r) = 2\pi ern(r)v(r). \qquad (3)$$

As was introduced by Meyer and Reif,[2] the mobility model is assumed. This means that the relation

$$v(r) = \mu E(r), \tag{4}$$

is applicable in the liquid where μ shows the mobility of the electron bubble. Using eqs.(2)~(4), one finds an equation,

$$rE(r)dE/dr + E(r)^2 - 2I/\mu = 0. \tag{5}$$

This equation is easily solved by replacing E(r) as F(r)/r and the following relations are obtained:

$$I = (\mu/2)(V_o/r_2)^2, \tag{6}$$

$$E(r) = (V_o/r_2)(r^2 - r_1^2)^{1/2}/r, \tag{7}$$

$$v(r) = \mu(V_o/r_2)(r^2 - r_1^2)^{1/2}/r, \tag{8}$$

$$n(r) = (V_o/4\pi e r_2)(r^2 - r_1^2)^{-1/2} \tag{9}$$

where V_o is the voltage difference between the cathode and anode and a condition $r_2 \gg r_1$ is used. To obtain eqs.(6)~(9), the field gradient dE/dr at r_1 is assumed to be zero as a boundary condition. It should be noticed that the field gradient at the vacuum tube cathode is usually zero and this boundary condition is satisfied if the cathode have an enough power of the

electron emission. A slight difference from the vacuum tube is that the gas sheath is regarded as a part of the cathode. This assumption seems to be appropriate because the electron mobility in the sheath is much larger than that in the liquid and the field gradient in the sheath may be substantially zero. It is also noted that there is a well known relation in the vacuum tube diode given by $I \propto V_o^{3/2}$ but it changes to $I \propto V_o^2$ in the liquid helium diode, as is shown by eq.(6). This is due to the fact that the ohmic assumption or the mobility model is used in liquid He II[7] while the free electron acceleration occurs in vacuum tubes.

§ 3. Bubble-Vortex Interaction

Taking logarism of eq.(6), one can get the relation,

$$\log_{10} I = \log_{10}(\mu/2) + 2\log_{10}(V_o/r_2), \qquad (10)$$

This means that the IV-curve in Fig. 1 should be linear if the mobility would be field independent. As an example, a theoretical line is drawn with the bubble mobility at 1.3 K determined by Meyer and Reif.[2] Roughly speaking, the resultant tangent of the experimental data is in accord with the theory but the absolute values are considerablly small. So we tried to explain the discrepancy by doing more systematic experiments. Fig. 4 shows a schematic view of the apparatus used in our study.

As the cathode filament, a commertially available tungsten wire with 9.1 μm in diameter and about 1 cm in length was used . The four terminal method was used for all electrical measurings as is usually done in semiconductor study because the electrical contact between the wire and copper lead was not always guaranteed because of the small diameter of the filament. The gas sheath around the wire is unstable when it is placed near the liquid surface[4] and the instability largely afects on the plate current so that almost of all measurements were done more than 10 cm below the liquid surface.

Fig. 5 shows the temperature dependence of the plate current I under a constant cathode-plate voltage. If the electron bubble were ruled by the bubble mobility, the current should decrease[2] under an increasing temperature of the liquid bath but it increases between 1.2 and 1.8 K. This result clearly indicates that the current can not be explained by the bubble mobility only. As another interaction in the liquid helium II in this temperature region, the bubble-vortex coupling should be taken into account.[8-9] Meyer and Reif pointed out[2] that the bubble mobility above 1 K is proportional to $\exp(-\Delta/kT)$, being Δ the roton energy, because the roton scattering process is the main origin of the bubble resistivity in liquid He II. In this paper, the notation μ_b is used for the bubble mobility due to this process. The effect of phonon scattering on the mobility is negligible in the present experimental conditions. Now the bubble-vortex interaction should be considered in the following way: the interaction does

not have a large effect when an external field is small but it gives a strong resistive force to the bubble motion giving rise a large mobility reduction.[10] The vortex trapping of bubble is very strong at low temperatures but it becomes weak when the liquid temperature increases presumably due to the decrease in vortex lifetime.[8] Considering these facts, the I-V-characteristics were investigated at various liquid temperatures and the main results are given in Fig. 6. Three theoretical lines assuming the bubble mobility μ_b are also shown. At low temperature, the difference is large but it becomes small as temperature increases and the agreement is fairly well at 1.76 K. Therefore, it is concluded that the bubble moves with bubble mobility μ_b near 1.7 K but the vortex trapping becomes large as temperature decreases.

A quantitative treatment of the field dependent mobility due to vortex trapping is calculated in the following way. First, we assume that all bubbles are trapped at r_1 because of a strong turbulent flow near the sheath surface. Then the vortex trapped bubbles move with a small mobility μ_v. However, a bubble in a vortex has an escape probability[11~12] which depends on the presence of the external electric field. Therefore, the bubble becomes free after a certain time elapse and it will move with a mobility μ_b after the escape. Cade[11] obtained the escape probability in the following form:

$$N/N_o = \exp\left[-\omega_o t \exp\left\{-(W_o - eEr_m)/kT\right\}\right], \qquad (11)$$

where N and N_o means the trapped bubble numbers at t=t, and t=0, respectively. The trapped energy W_o(45 K), the effective radius r_m under an electric field E (35 Å), and the characteristic frequency ω_o(7 x 10^{12}cps) were determined considering their results.[11~12)]

The field dependent resultant mobility μ^* is now can calculate by connecting two mobility regions. The average velocity $\langle v \rangle$ is

$$\langle v \rangle = r_2/(t' + t'') = r_2/\left\{(r'/\mu_v E) + (r_2 - r')/(\mu_b E)\right\}, \quad (12)$$

where t' and t'' mean flight times with μ_v and μ_b, respectively and r' is the flight distance under the trapped state. These values are calculated by using eq.(11) and μ^* is obtained as

$$\mu^* = \mu_v/\left\{(1 - \mu_v/\mu_b)(1 - \exp(-z))/z + \mu_v/\mu_b \right\}, \quad (13)$$

$$z = (r_2\omega_o/\mu_v E)\exp\left\{-(W_o - eEr_m)/kT\right\}, \quad (14)$$

Fig. 7 shows the comparison between the theoretical curve given by eq.(13) and the experimenral results, assuming the ratio μ_v/μ_b to be 7.8. A good agreement was obtained as is seen in the figure. An adjustable parameter μ_v is usually very difficult to obtain precisely.[10)] It is noticed that the IV-curve approaches to the pure bubble motion line both in the lower and higher field region. This is explained as follows: in the low field region, the bubble has much chance of escape because of the long drift time while the escape probability becomes large when the field becomes strong.

§ 4. Roton Creation Process Under a Strong Field

A new property of IV-characteristic was obtained when the electric field was increased up to about 20 kV/cm, as is seen in Fig. 8. The current becomes flat near 8 kV/cm and again increases at 20 kV/cm region. The results can be explained in the following way. In usual bubble roton scattering, the roton creation process does not occur because the kinetic energy of the bubble is not so large. However, the bubble will be able to make another new roton if the velocity exceeds the critical value v_c determined by

$$\Delta = (1/2)M^* v_c^2 , \qquad (15)$$

where Δ is the roton energy and M^* is the effective mass of bubble. v_c obtained from eq.(15) is about 60 m/sec. It is usually accepted that the drift velocity of bubble does not exceed v_c.[10] However, it is pointed out that the bubble has an enough energy to make new roton under an electric field of about 10 kV region because the escaping bubble from the vortex can get more energy than Δ during the free acceleration time. The critical electric field E_c to realize this condition is given by

$$(1/2)M^* v_c^2 = eE_c\langle L\rangle, \qquad (16)$$

where $\langle L\rangle$ is the mean free path of the bubble and it is easily calculated by using Meyer and Reif's formula.[2] The result shows

that E_c is about 5 kV at 1.3 K. Therefore the roton creation process will occur near this voltage giving rise a decreasing tendence of the resultant mobility in accord with the experimental results given in Fig. 8. Then the resultant mobility written by μ_{b+r} should be reduced considerablly, as in Fig. 8. The roton creation process is ascertained by investigating the temperature dependence given in Fig. 9. As temperature increases, the mean free path decreases so that the critical field E_c increases in accord with the experiment although the quantitative treatment is difficult.

As a conclusion, the IV-characteristic of the diode can be summalized as is shown in Fig. 10. In the region A, bubble moves with the mobility μ_b coming from the simple roton scattering but the bubble-vortex interaction should be taken into account in the region B. In the region C, the escape probability from the vortex becomes large so that the current again approches to the μ_b line. Spangler et al.[3] measured in the B and C regions and their results show a good coincidence to ours. A new interaction occurs in the region D and the resultant mobility goes down to μ_{b+r} line, namely, the mobility due to the roton creation process in addition to the usual roton scattering.

It is noticed finally that the average bubble density in the diode is considerably high and it seems to be useful for wide experimental studies of the electron bubbles. The average is easily calculated from eq.(9) and it becomes to 10^{10}/cc at V_o/r_2=3 kV and also becomes to 10^{11}/cc at 30 kV.

References

1) G. Careri, J. Reuss, F. Scaramuzzi and J.O. Thomson: Proc. LT-5 (Wisconsin)(1957) 79, Nuovo Cimento (B) 13 (1959) 186.

2) L. Meyer and F. Reif: Phys. Rev. 110 (1958) 279, Phys. Rev. Letters 5 (1960) 1, Phys. Rev. 119 (1960) 1164.

3) G.E. Spangler and F.L. Hereford: Phys. Rev. Letters 20 (1968) 1229.

4) M. Date, H. Hori, K. Toyokawa, M. Wake and O. Ichikawa: LT-13 (Boulder)(1972),
M. Date, H. Hori and O. Ichikawa: to be published in J. Phys. Soc. Japan.

5) K. Okuda, Y. Inaba and M. Date: to be published in J. Phys. Soc. Japan.

6) M.H. Nichols: Phys. Rev. 57 (1940) 297.

7) P.V.E. McClintock: Phys. Letters 29A (1969) 453.

8) For example, F. Reif: Proc. LT-10 (Moscow)(1966) 86.

9) D.M. Sitton and F.E. Moss: Phys. Rev. Letters 23 (1969) 1090.

10) D.L. Goodstein, U. Buontempo and M. Cerdonio: Phys. Rev. 171 (1968) 181.

11) A.G. Cade: Phys. Rev. Letters 15 (1965) 238.

12) P.E. Parks and R.J. Donnelly: Phys. Rev. Letters 16 (1966) 45.

Figure Captions

Fig. 1. IV-characteristic of a diode in liquid helium II first observed by Spangler et al.[3] A straight μ_b line is drawn by eq.(10) under an assumption that the mobility is determined by the roton scattering only.

Fig. 2. Cut view of the diode.

Fig. 3. Radial dependences of the electric field E and electron bubble density n in arbitrary scale. $\langle n(r) \rangle$ means the average.

Fig. 4. Schematic view of the apparatus. Four terminal contacts for the filament are not shown.

Fig. 5. Temperature dependence of the plate current under a constant voltage.

Fig. 6. IV-characteristic at three temperatures. The straight lines show theoretical curves based on the constant bubble mobility model.

Fig. 7. (A) Theoretically deduced curve of the potential energy of an electron bubble in a vortex as a function of its distance r from the vortex center in the presence of a electric field of 1 kV/cm. (B) IV-characteristic curve in the vortex trapped region. A straight line is the IV-curve without vortex interaction while the other curved line is written using the mobility in eq.(13). Open circles show the experimental results.

Fig. 8. IV-curve under a strong electric field. Dotted lines show the experimental results done by Spangler et al.[3]

Fig. 9. Temperature dependence of high field IV-curve.

Fig. 10. Schematic view of total IV-curve.

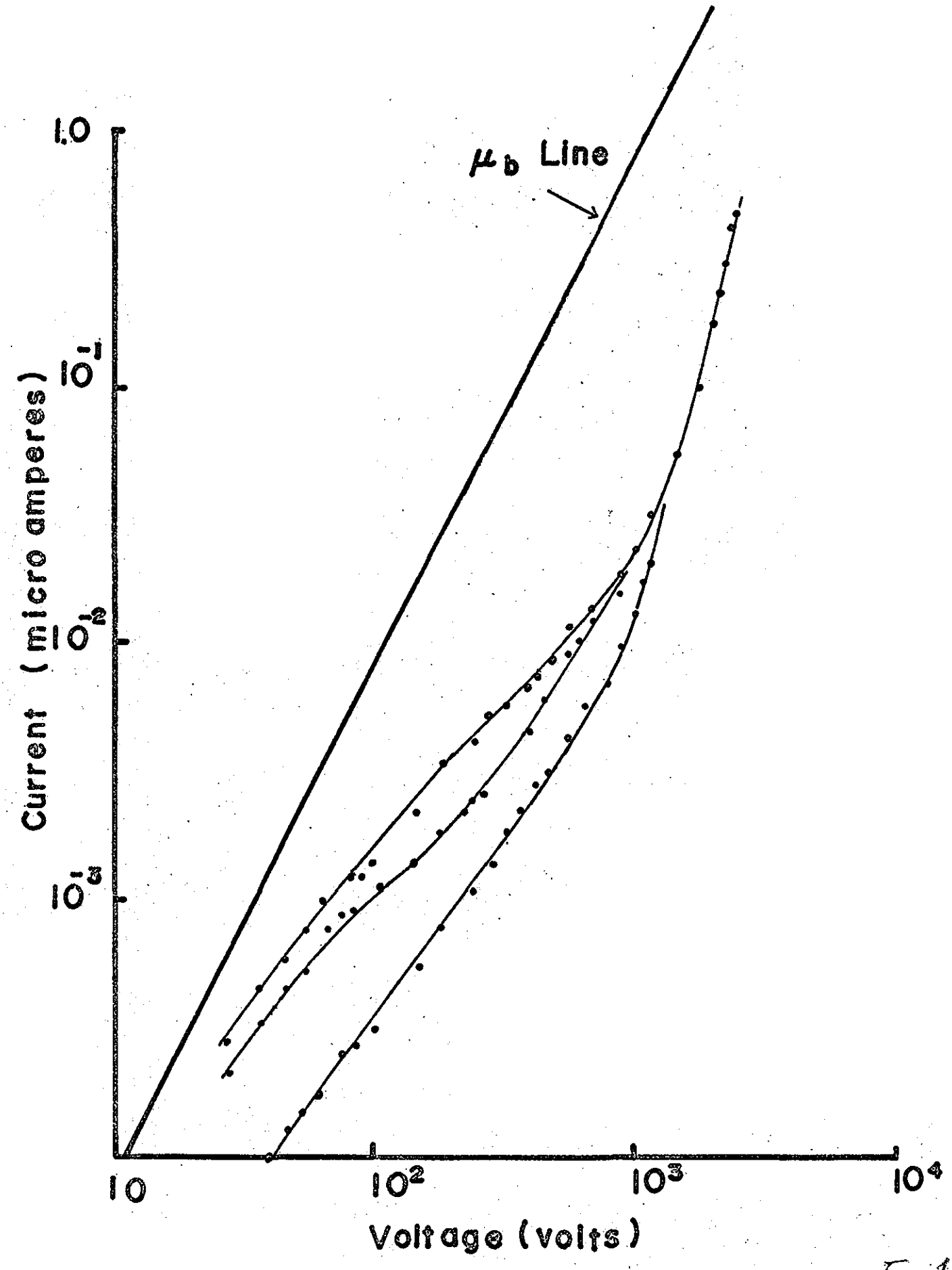
1.0
μ_b Line
Current (micro amperes)
10^{-1}
10^{-2}
10^{-3}
10
10^2
10^3
10^4
Voltage (volts)

Fig. 1

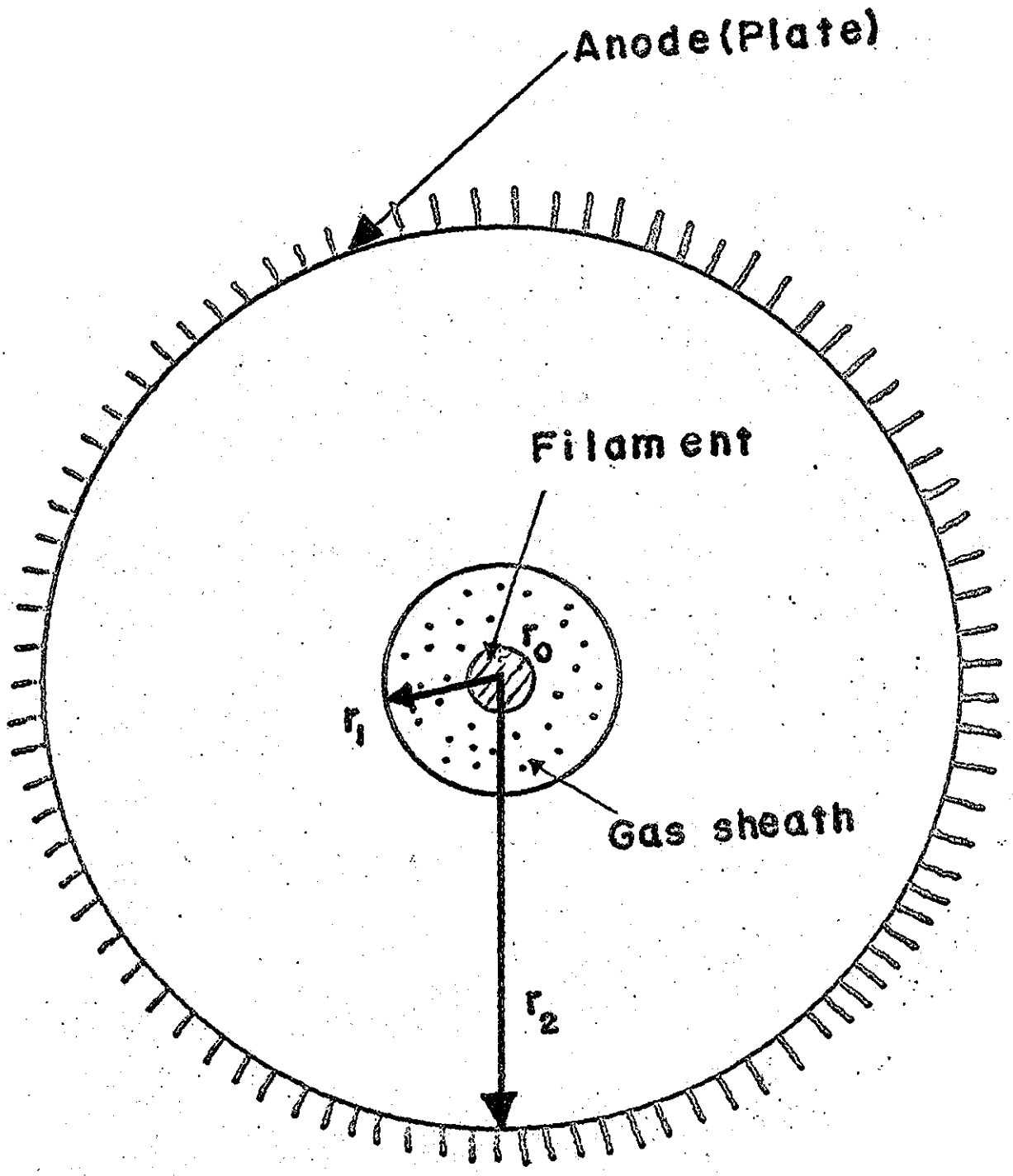

Fig. 2

Fig. 3

Fig. 4

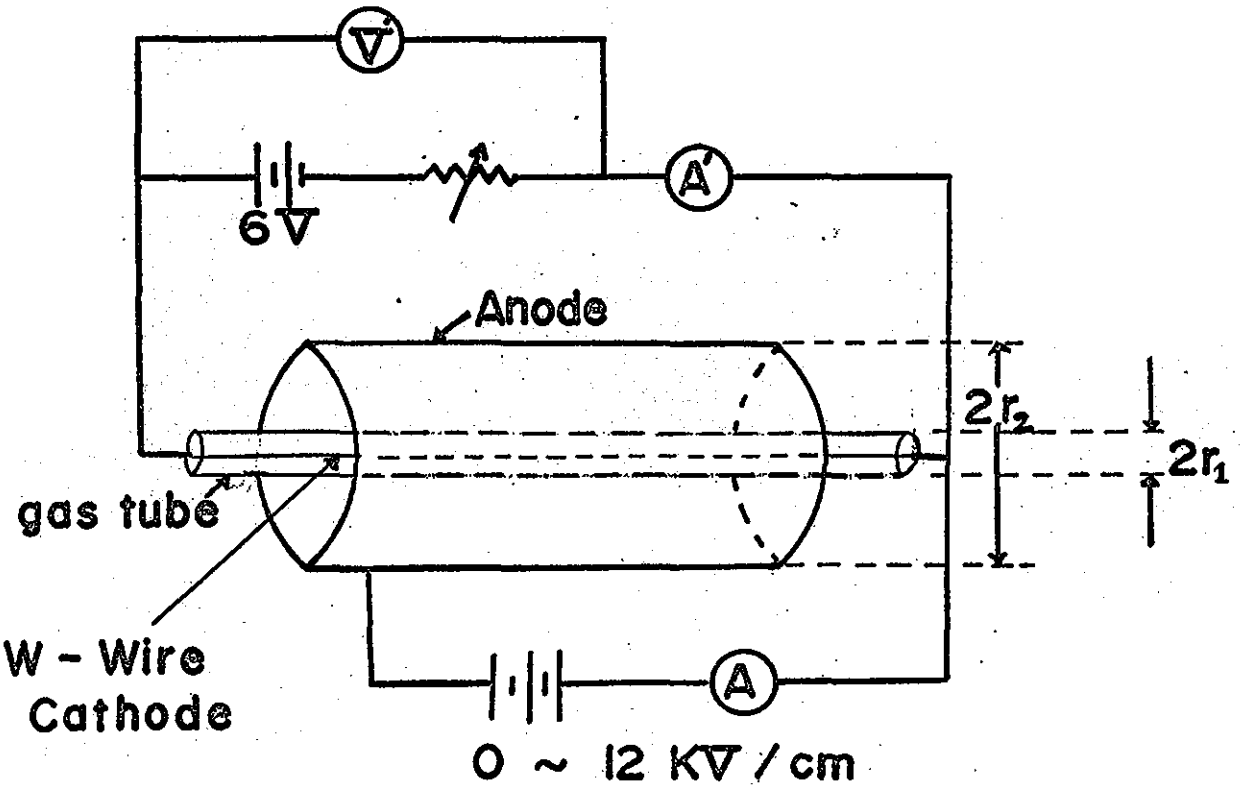

Fig.5

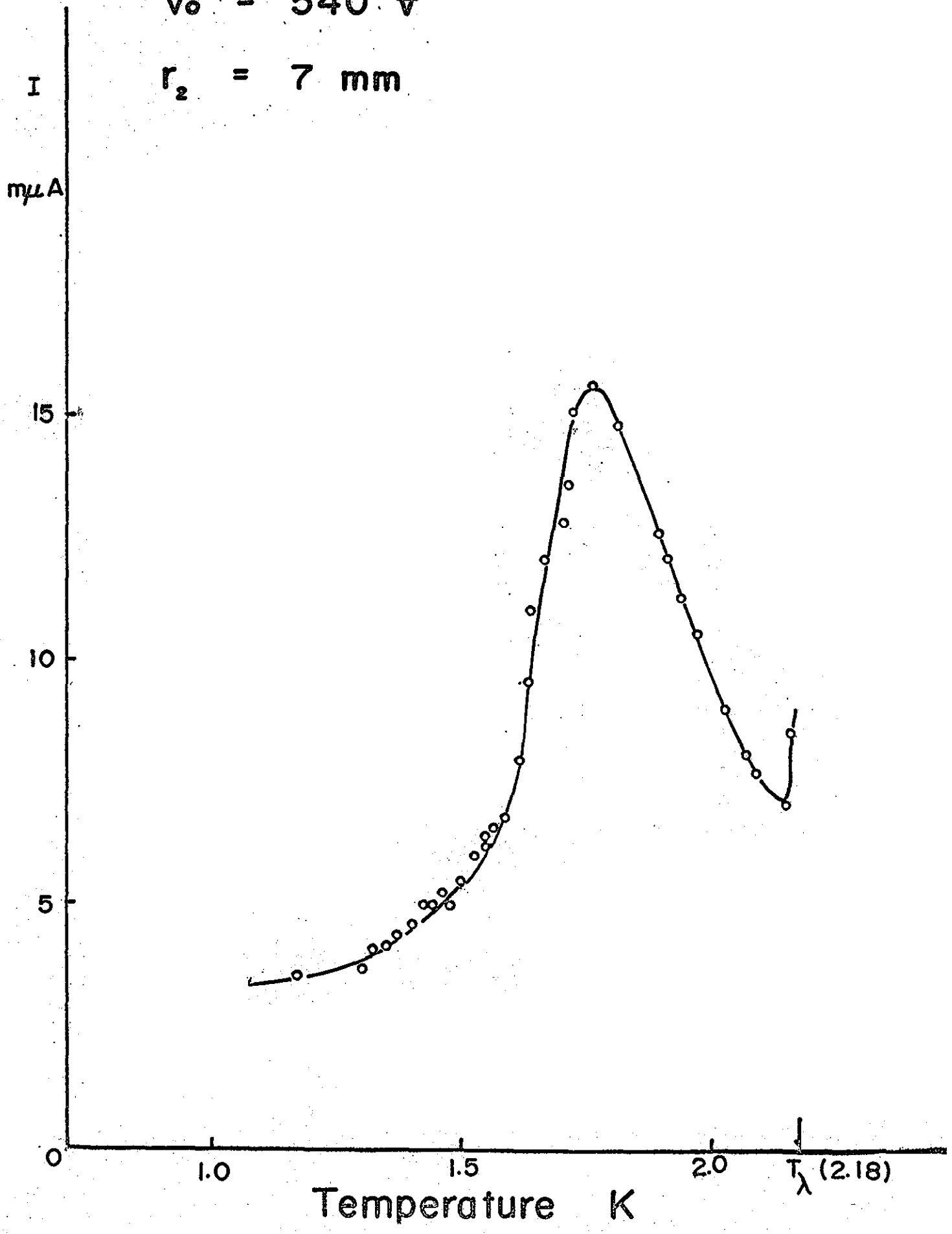

Fig. 6

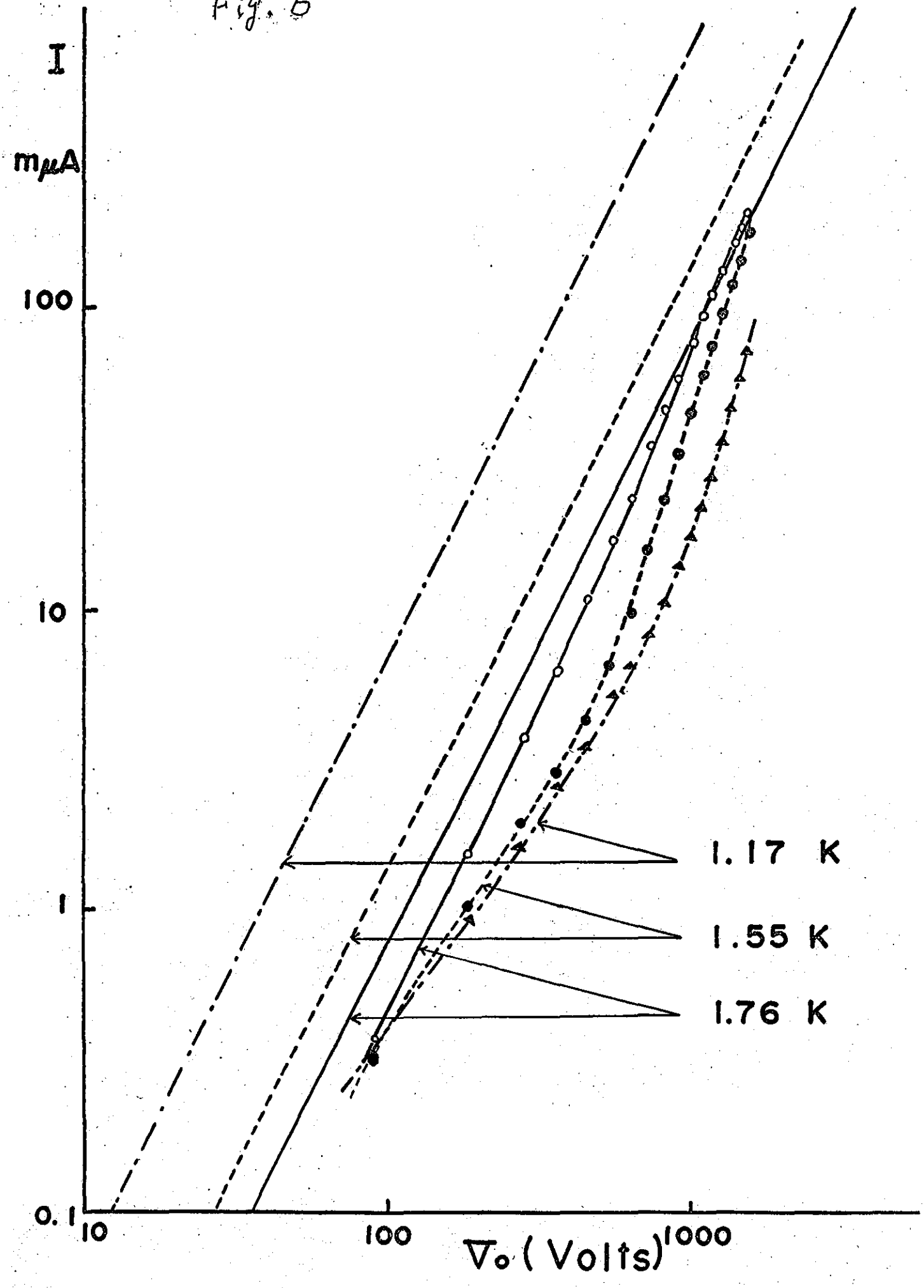

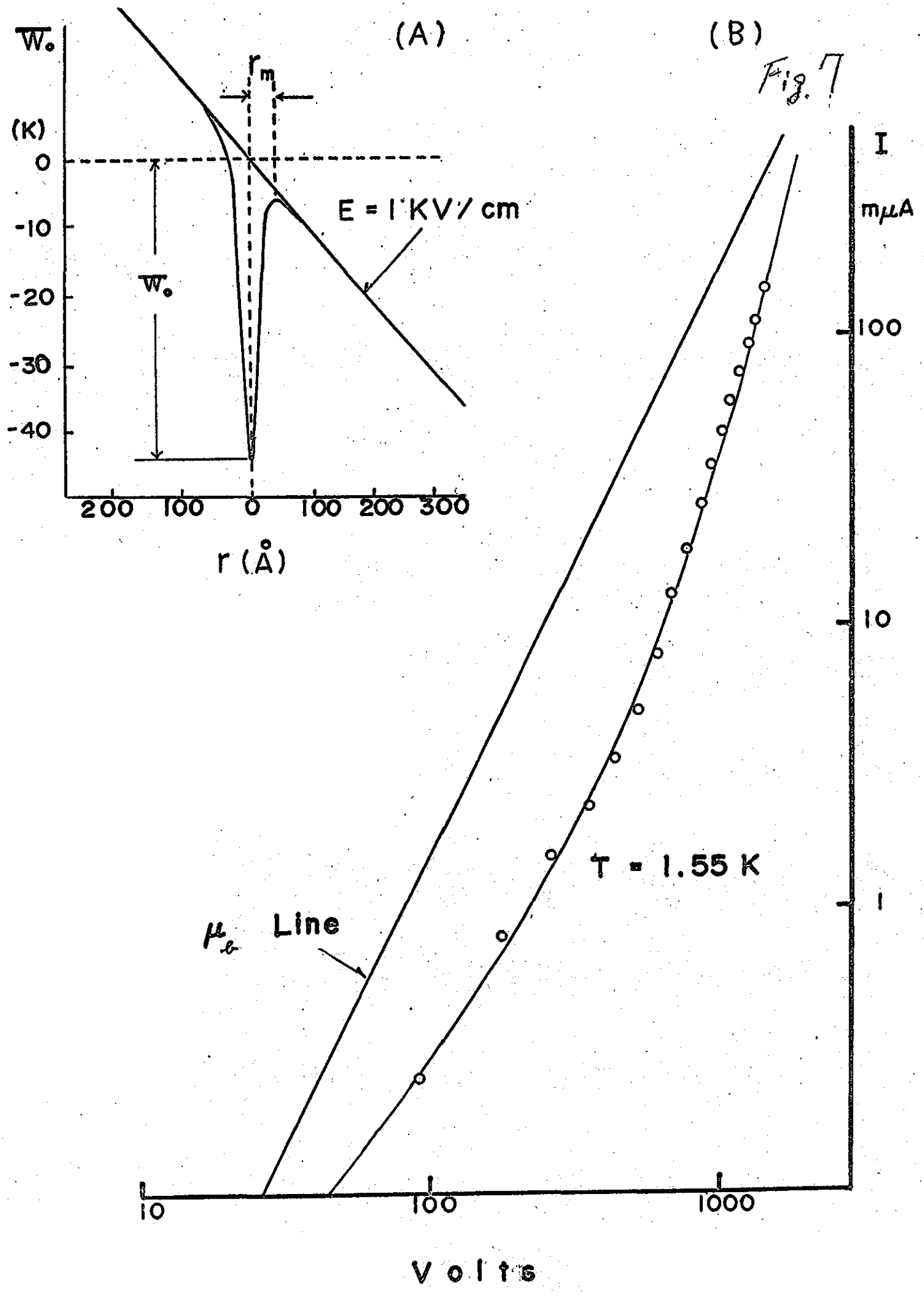
(A)
(B)
Fig. 7
W₀
(K)
0
-10
-20
-30
-40
rm
W₀
E = 1 KV/cm
200
100
0
100
200
300
r (Å)
I
mμA
100
10
1
T = 1.55 K
μb Line
10
100
1000
Volts

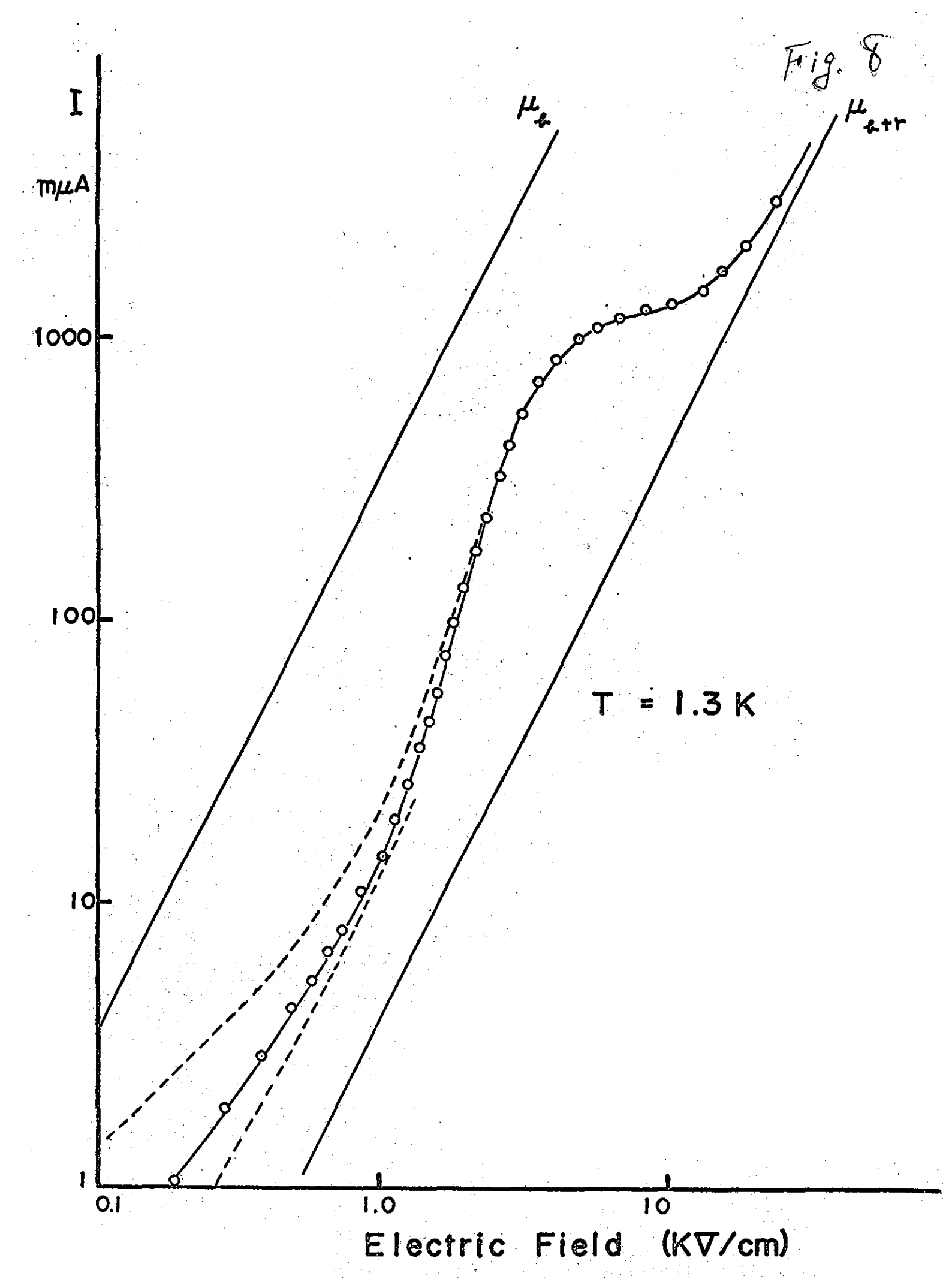
Fig. 8
I
mμA
1000
100
10
1
μ_{drift}
μ_{extr}
T = 1.3 K
0.1
1.0
10
Electric Field (KV/cm)

Fig. 9

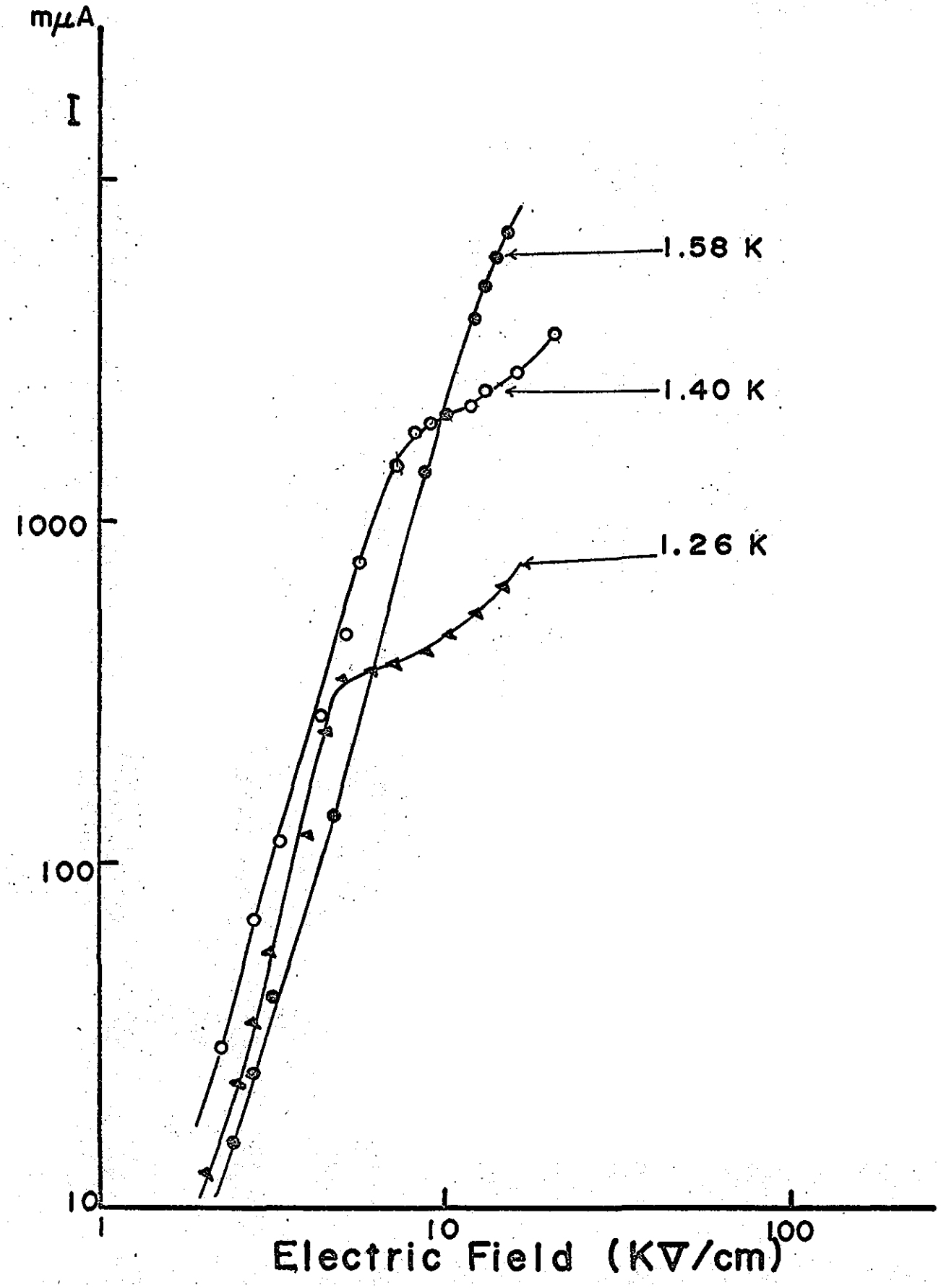

Fig. 10

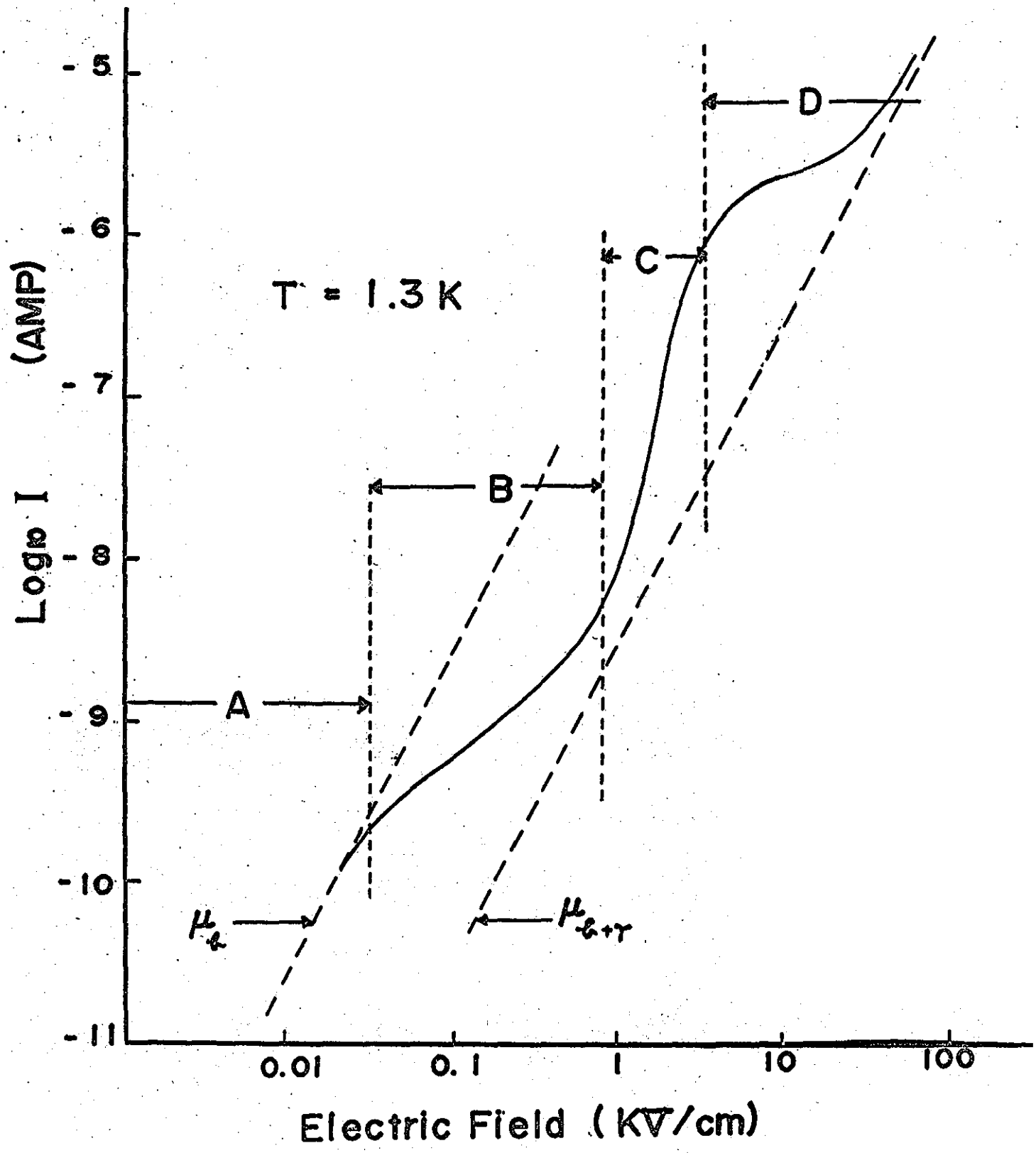
-5
-6
-7
-8
-9
-10
-11
Log₁₀ I (AMP)
T = 1.3 K
A
B
C
D
μ_e
μ_{e+T}
0.01
0.1
1
10
100
Electric Field (KV/cm)

PART III

Charge Carriers in Liquid He II Produced by Spark Discharge

Abstract

A New methods of producing various charge carriers and neutral impurities in liquid He II were developed by making a spark discharge plasma just above the liquid surface. This method can produce + or - charge carriers of 10^{11}/cc and the optical and transport properties of these cahrge carriers were invesitgated. It was found that the plasma in the liquid shows a strong recombination effect by the irradiation of light having an energy larger than W_o, where W_o(0.6 eV) is the dissociation energy of an electron from the electron bubble.

§ 1. Introduction

The injection of excess charge carriers into liquid He II was done by Careri et al.[1] and shortly after that Meyer and Reif established the mobility model[2] based on the roton and phonon scattering mechanisms. They used a radioactive isotope Po^{210} as an ion source. α-particles emitting from the isotope produce both + and - ions in He II and almost all important experimental results have been obtained by using this method. It is now well known that the majority part of negative charge carriers are electrons in the bubble state[3] while the positive ions such as He^+ form so called iceberg or snowball state.[4] The effective mass was estimated to be 100~200 M_{He} for the bubble and about 50 M_{He} for the iceberg,[4] where M_{He} means the atomic mass of He. The electronic states of the electron bubble were investigated by several groups[5,6] but they are not so clear yet. The surface bound state of electrons was recently observed[7~9] including cyclotron resonance phenomena.[10] Of transport properties of + and - carriers in He II, vortex lines and vortex rings play ~~an~~ important roles on the drift velocity and the charged vortices were investigated from various point of view.[11]

The isotope method mentioned above can supply only about 10^5 ~10^7/cc of charged particles in liquid so that it is not enough to develope the extensive studies such as the optical absorption or spin resonance. Therefore, various new methods to obtain high density charge carriers were tried by many groups. In 1968, Spangler and Hereford[12] obtained about 10^9/cc of electron bubbles

by using a hot tungsten filament immersed in the liquid He bath. In the same year, we initiated to get a dense charge carriers by the spark discharge method[13] and obtained more than 10^{10}/cc in liquid He II. In 1969, Onn and Silver[14] made a new source of electrons in He II by the field emission method using a cold cathode emitter of Al-Al_2O_3-Al diode and obtained about 10^9/cc electron bubble density. An other field emission method was developed by Halpern et al.[15] and also by McClintock[16] to obtain considerable amount of electron bubbles. Although it is not so effective to have high carrier density, photo electron production due to light irradiation was tried by Woolf et al.[17] by using commertially available photo tubes and this method was also tried by the present authors[13] by the UV irradiation on Na films. Recently, an effective new method to produce various kinds of charged particles and neutral impurities was developed by Dennis et al.[18] who injected high speed electrons into the liquid He bath through a thin metal foil. This electron beam excitation of liquid He made possible the first spectroscopic investigation of the excited states of liquid He. They found that there are many neutral excitations such as excited He atoms and excited diatomic He molecules as was first suggested by Surko and Reif.[19]

As is mentioned above, the spark discharge techniques developed by our group can be considered one of the most useful method to produce high density charge carriers in liquid He II and the detailed procedure and the main results will be shown in the present paper.

§ 2. Experimental Procedure

The schematic diagram of the spark discharge method used in our laboratory is shown in Fig. 1. It consists of the discharge electrodes A and B in the helium gas and a collector plate C in liquid. Sometimes a light shutter D was inserted to prevent the visible or UV light produced by the discharge plasma and a grid G was frequently used to control the current. In the early stage of the experiment, the AC source was used for E_1 as well as the DC source but the latter was more stable with lower noise so that most of all experimental results were obtained by using a battery of 100～300 V. Care should be paid to keep the dissipated power to be within 0.2～2 watts for the discharge for avoiding the undesirable evaporation of liquid helium. It was hard to get a stable discharge below 0.2 watts. The plus or minus charge current was obtained in the liquid by applying a DC voltage E_2 between plates B and C. Fig. 1 shows a case where the + charge current is introduced. A typical example of the IV characteristic of the discharge plasma and the plate current between B and C are shown in Fig. 2 where the plate current was measured when the plate C was one centimeter below the liquid surface. As will be shown later, the plate current strongly depend on the liquid helium depth and temperature. The maximum plate current thus obtained was about 10^{-6} ampere which is larger than that of the hot cathode method developed by Spangler et al.[12]. The spark discharge method can also be used as an ion source of various kind atoms by supplying other materials into the plasma.

§ 3. Ionized and Neutral Excitations in the Gas Plasma

Before going to discuss various behaviors of the charge carriers in the liquid bath, it is necessary to investigate many excited states produced by the spark discharge because the composition of the gas plasma strongly affects on the properties of charge carriers in the liquid. So we tried to investigate the discharge phenomena just above the liquid surface by the spectroscopic method.

It is well known that the spark discharge in helium gas at high temperatures produces various kinds of neutral excitations such as the excited states of He atom or the diatomic molecules in addition to the charged particles. Of these excited states, care should be paid to two metastable states, 2^3S and $a^3\Sigma_u^+$, the atomic and diatomic triplet states, respectively. The concentrations of these states are expected to be large because the life times of these states are very long. We observed various spectra coming from the plasma near the liquid surface and an example of the data is shown in Fig. 3, in which the typical pattern of symmetric diatomic rotational spectra is given. The excited states or particles in the plasma can be classified into five groups, i.e., the neutral excited helium atom He^*, neutral excited diatomic molecule He_2^*, ionized atom He^+, ionized diatomic molecule He_2^+, and free electrons. The density of other ions such as He^{2+} were negligibly small.

During the preliminary experiment of the spark discharge method,[13] it was simply believed that the charged particles

in liquid could easily be supplied from the discharge plasma into the liquid by applying an electric field E_2. However, this idea was found to be too simple to explain the experiment. We found that the plate current between B and C becomes very small after the light shutter D is inserted. This fact is difficult to explain from the simple model because the mean free path of the charge carriers under our experimental condition is of the order of μm so that the shutter which consists of two layers of the macroscopic lattice should not largely afects on the plate current. However, the current decreases down to 10^{-11} ampere which is about 10^{-3} smaller than the normal current. Such a discrepancy was removed by introducing a new mechanism of generating charge carriers into the liquid. Instead of the direct plunge of charged particles, we consider the diffusion of excited neutral particles from the gas plasma into the liquid. These particles then ionize by the irradiation of UV light produced by the discharge process. This process also produces visible light but its effect was found to be not so important. This conclusion was obtained by changing various kinds of light filters as an optical shutter D. Our conclusion is also consistent with the experimental results of surface barriers[7~9] for charged particles at the liquid helium surface.

One more support of our model was obtained by estimating the density of various particles in the plasma. Under usual discharge condition, densities of helium ion, diatomic helium ion, neutral diatomic molecule, and electron were estimated to be

He^+: 6 x 10^7/cc, He_2^*: 1 x 10^{13}/cc, and He_2^+ and electron: 3 x 10^{12}/cc, respectively. These values were obtained by comparing the corresponding spectrum intensities with their matrix elements[20] and the electron density was determined by the charge neutrality. Although these values are not so precise and show only the order, it is noticed that the number of neutral molecules is much larger than those of the charged particles because of the presence of metastable state.

§ 4. Charge Carriers in Liquid He II

As is mentioned in the previous section, the plate current depends strongly on the liquid helium depth and two typical examples of the depth dependence for + and - carriers are shown in Fig. 4. The + current flow was larger than that of the - ion in accord with the iceberg and bubble models for these ions. As these ions are supplied by the ionization of thermally diffused neutral particles in the liquid bath, the decreasing ratio of plate current when the plate depth inceases so large that the exact value of the Plate current below 5 cm was hard to obtain. As is seen in the figure, the depth dependence becomes flat when the liquid is shallow and this was explained by the space charge effect near the surface, as will be seen later. An interesting fact is that the current does not show an abrupt increase due to the discharge effect just above the surface of the liquid when the positive ions are pulled by the plate while a strong discharge effect occurs between B and C when - ions are pulled.

This curious effect was explained as follows: the plate C above the liquid surface is usually covered by a thin film of superfluid helium and the film acts as a protector for the electrical discharge. This assumption was ascertained by controlling supply of liquid to the film by changing the diameter of supporter rod of the plate. When the diameter was small, the liquid He supply from the bath to film along the rod surface was strongly limitted so that the discharge occured so easily, as expected. In the case of negative ion collector, i.e., when the plate C is positive, electrons having high energy in the gas plasma collide with the plate giving rise the evaporation of many helium atoms from the film so that the plate exposes out of the insulating liquid.

To estimate the spacial distribution of the charge carrier density in liquid, a grid G in Fig. 1 was inserted as a test probe moving across the liquid surface and it was found that the density is extremely large near the surface. Moreover, it was also found that the spark discharge produces an automatic polarization even when the plate voltage between B and C goes to zero, as is schematically shown in Fig. 5(b). This means that the positive ions are rich in liquid while the negative charges in gas are excess making an electrical double layer around the boundary surface. This fact was ascertained by measuring a spontaneous electrical current appeared between grid and plate under a condition that the plate and grid system is perfectly isolated from the discharge plates A and B.

Fig. 5(a) shows an example of the spontaneous current as a function of the grid position. The plate is placed about 10 cm below the liquid surface. When the grid crosses the surface, a drastic change of the current occurs as is seen in Fig. 5(a) and the result supports the charge distribution model given in Fig. 5(b). The maximum charge density near the surface was of the order of $10^{11}\sim10^{13}$/cc both above and below the surface. It is believed that photo electrons from the liquid bath are produced above the surface by the irradiation of UV light coming from the discharge plasma, although such an assumption is very difficult to verify directly.

§ 5. Negative Photo Conductivity due to Recombination of Charge Carriers

When + and - charge carriers coexist in the liquid bath, the recombination of these carriers can be expected. The first experiment of the recombination was done by Careri et al[21] using a method of direct impact between + and - carriers. Although the bubble and iceberg models for the charged particles in liquid He II were not established at that time, they substantially determined the collision crossection of these particles.

Recently, we found that the recombination is strongly enhanced by the irradiation of light and as the result a negative photo conductivity occurs in the charge plasma in liquid because of the decrease in resultant charge density. After the first discovery of the negative photo conductivity by a white light,

we tried to obtain the wave length dependence of the irradiated light using an optical monochrometer from the infrared to visible regions. The result is shown in Fig. 6. The recombination effect becomes large as the photon energy increases. It is noticed that there is a threshold energy near 0.6 eV (2 μm) below which the negative photo conductivity, i.e., the recombination of + and - carriers does not occur.

Considering these experimental results, we introduced a new model to explain the recombination enhancement due to light. For an electron trapped in a bubble, it has been believed that the trapping energy is of the order of 1 eV. This was suggested by Northby and Sanders[5] and shortly after that Fowler and Dexter[6] theoretically indicated that the energy from 1s level to the continium state is slightly less than 1 eV. Recently, Rayfield and Schoepe showed that the energy can be estimated to be 0.7 eV. Noticing the fact that our threshold energy is close to these value, it is easily concluded that electrons in the liquid bath become free from the bubble by irradiation of light having the energy higher than 0.6 eV. As the ejected electrons can move so fast in liquid before going down to the next bubble state that the recombination probability with coexisted positive ions will be enhanced largely, giving rise a strong negative photo conductivity in the system.

References

1) G. Careri, J. Reuss, F. Scaramuzzi and J.O. Thomson: Proc. LT-5 (Wisconsin)(1957) 79, Nuovo Cimento (B) 13 (1959) 186.

2) L. Meyer and F. Reif: Phys. Rev. 110 (1958) 279, Phys. Rev. Letters 5 (1960) 1, Phys. Rev. 119 (1960) 1164.

3) K.R. Atkins: Phys. Rev. 116 (1959) 1339.

4) A.J. Dahm and T.M. Sanders,Jr.:Phys. Rev. Letters 17(1966)126.

5) J.A. Northby and T.M. Sanders,Jr.: Phys. Rev. Letters 18(1967) 1184.

6) W.B. Fowler and D.C. Dexter: Phys. Rev. 176 (1968) 337.

7) L. Brushi, B. Maraviglia and F.E. Moss: Phys. Rev. Letters 17 (1966) 682.

8) R. Williams, R.S. Crandall and A.H. Willis: Phys. Rev. Letters 26 (1971) 7.

9) R.S. Crandall and R. Williams: Phys. Rev. A5 (1972) 2183.

10) T.R. Brown and C.G.Grimes: presented to LT-13(Boulder)(1972).

11) For example, F. Reif: Proc. LT-10 (Moscow) (1966) 86.

12) G.E. Spangler and F.L. Hereford: Phys. Rev. Letters 20(1968)1229.

13) M. Date: Low Temperature Symposium, J. Phys. Soc.(Nagoya)(1968), M. Date, H. Hori and H. Kamata: Proc. LT-12 (Kyoto) 93.

14) D.G. Onn and M. Silver: Phys. Rev. 183 (1969) 259.

15) B. Halpern and R. Gomer: J. Chem. Phys. 51 (1969) 1031.

16) P.V.E. McClintock: Phys. Letters 29A (1969) 453.

17) M.A. Woolf and G.W. Rayfield: Phys. Rev. Letters 15 (1965)235.

18) W.S. Dennis, E. Durbin,Jr.,W.A. Fitzsimons, O. Heybey and G.K. Walters: Phys. Rev. Letters 23 (1969) 1083.

19) C.M. Surko and F. Reif: Phys. Rev. Letters 20 (1968) 582.

20) G. Herzberg: Molecular Spectra and Molecular Structures, van Nostrand Reinhold Co. Ltd.(1950).

21) G. Careri and F. Gaeta: Nuovo Cimento 20 (1961) 1461.

22) G.W. Rayfield and W. Schoepe: Phys. Letters 37A (1971) 417.

Figure Captions

Fig. 1. Schematic diagram of the spark discharge method. Liquid temperature was controlled by vapor pressure. E_1 was between 100 ~ 300 V and 0 ~ 1 kV for E_2. The control grid G was connected with a suitable bias voltage to B and C.

Fig. 2. I-V characteristics of the discharge between A and B (cross points) and the plate current between B and C(open circles) when the positive ions are pulled by the plate C.

Fig. 3 Examples of He_2 spectra showing well resolved rotational structures.

Fig. 4. Plate currents as a function of the liquid depth. Vertical dotted lines show the position where the undesirable spark discharge occurs between B and C.

Fig. 5 (a) Grid current as a function of the liquid depth in an arbitrary scale. (b) Schematic view of the charge distribution near the liquid surface.

Fig. 6. Coefficient of the negative photo conductivity as a function of photon energy(arbitrary scale).

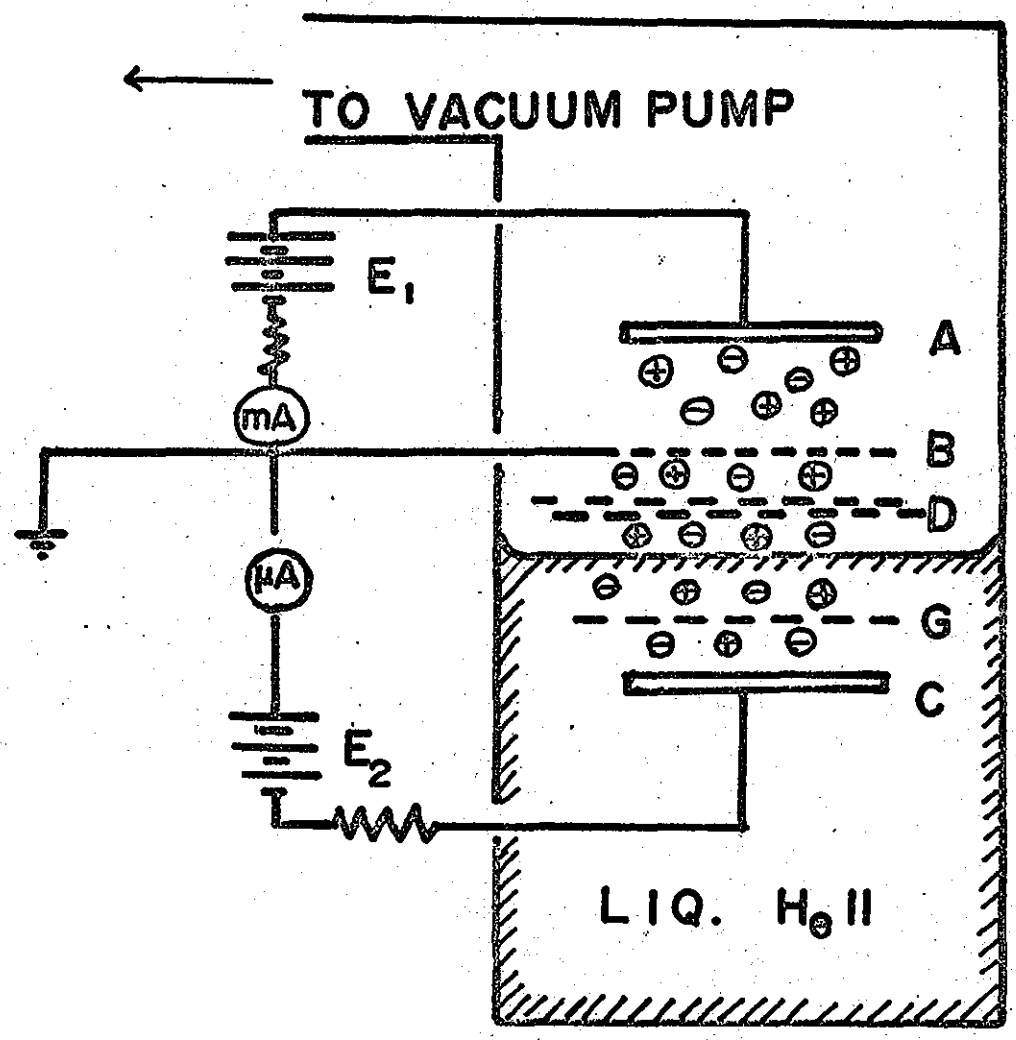

Fig. 1

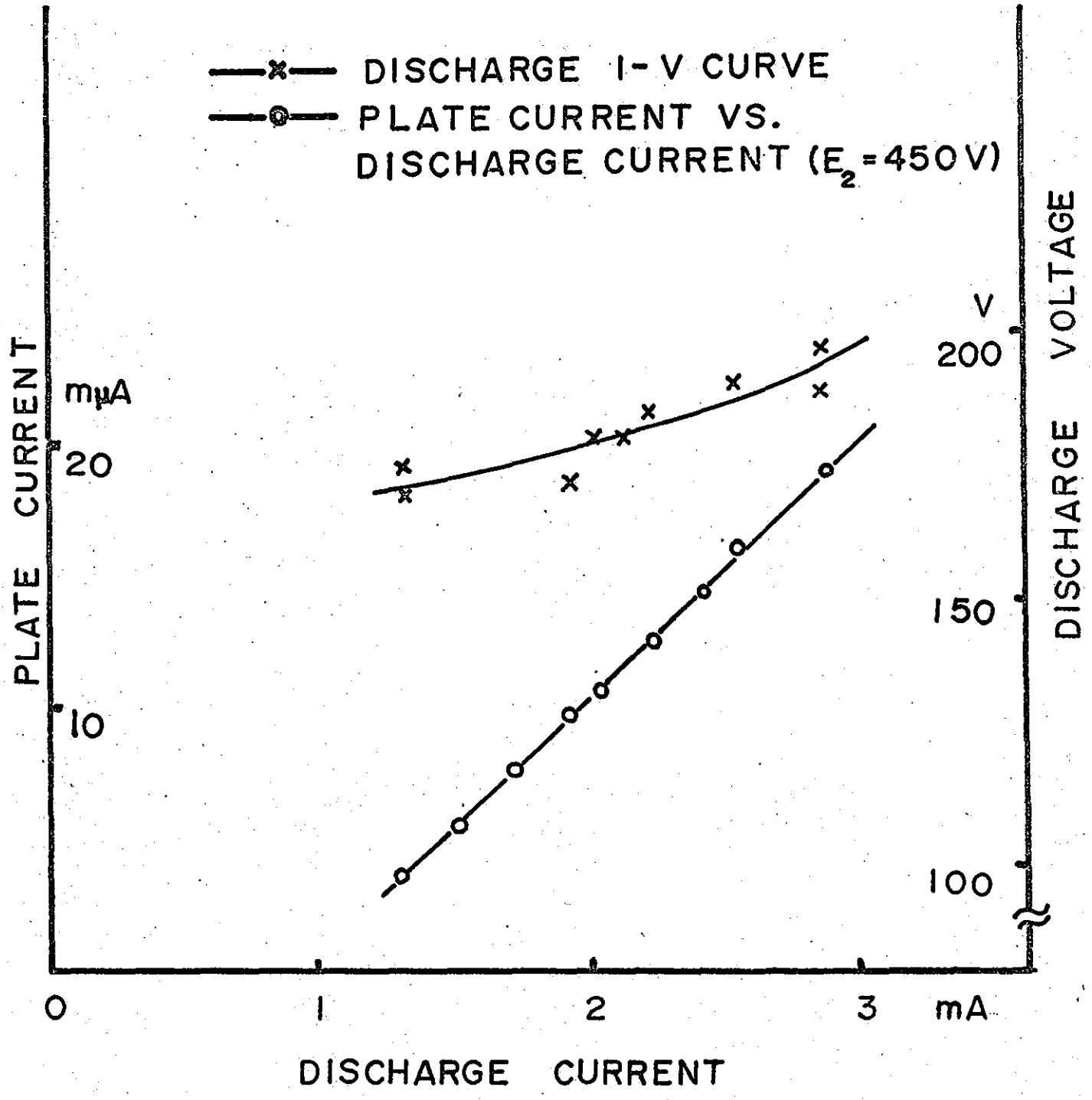
DISCHARGE I-V CURVE
PLATE CURRENT VS.
DISCHARGE CURRENT (E_2=450V)
PLATE CURRENT
mμA
20
10
V
200
150
100
DISCHARGE VOLTAGE
0
1
2
3
mA
DISCHARGE CURRENT

Fig. 2

Fig # 3

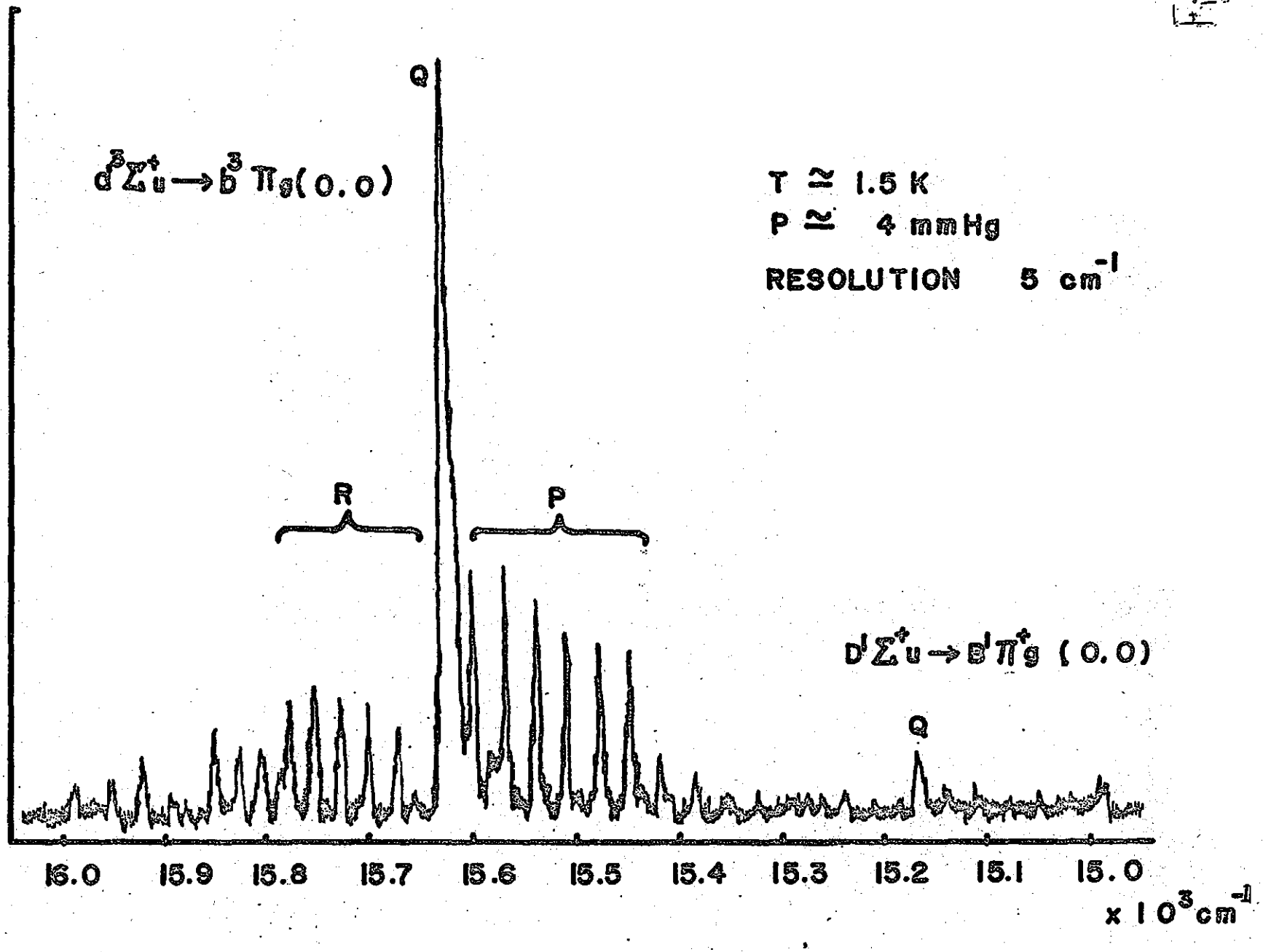
Q
$d^3\Sigma^+_u \rightarrow b^3\Pi_g(0.0)$
T ≃ 1.5 K
P ≃ 4 mmHg
RESOLUTION 5 cm^{-1}
R
P
$D'\Sigma^+_u \rightarrow B'\Pi^+_g$ (0.0)
Q
16.0
15.9
15.8
15.7
15.6
15.5
15.4
15.3
15.2
15.1
15.0
x 10^{3}cm^{-1}

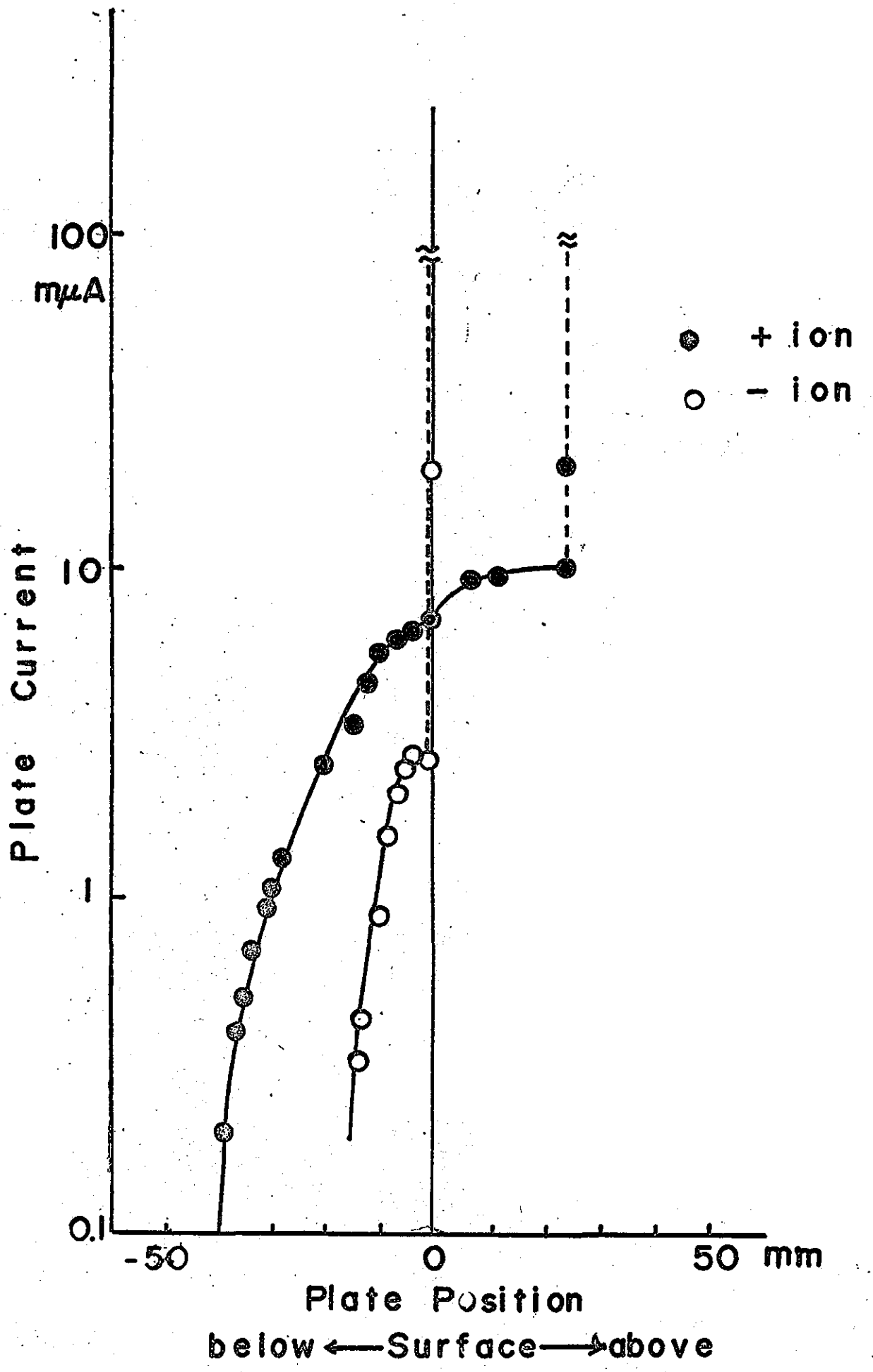
100
mμA
10
1
0.1
Plate Current
+ ion
− ion
-50
0
50 mm
Plate Position
below ← Surface → above

Fig 5(d)

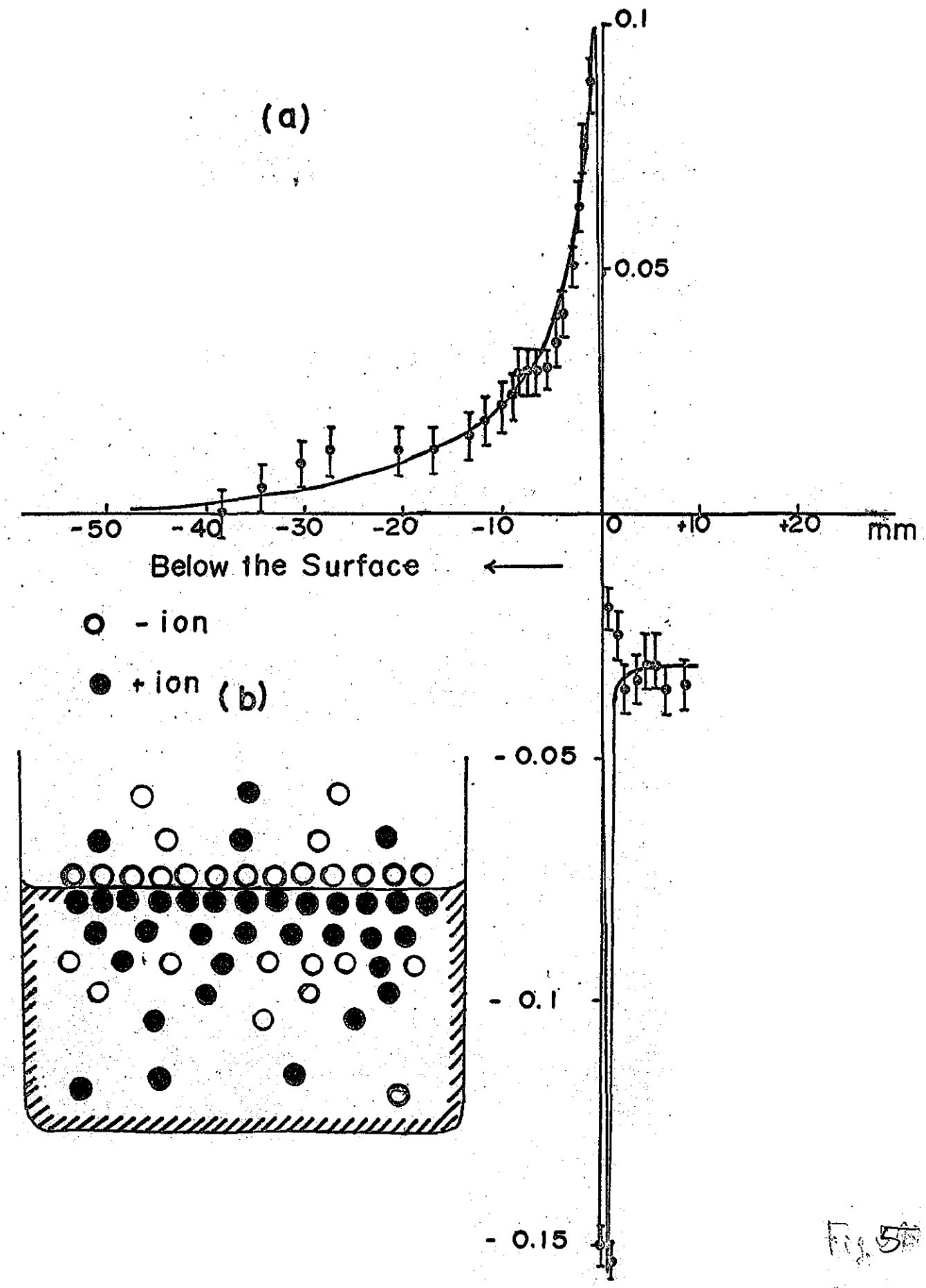
(a)
0.1
0.05
-50
-40
-30
-20
-10
0
+10
+20
mm
Below the Surface
- ion
+ ion
(b)
- 0.05
- 0.1
- 0.15

Fig. 5

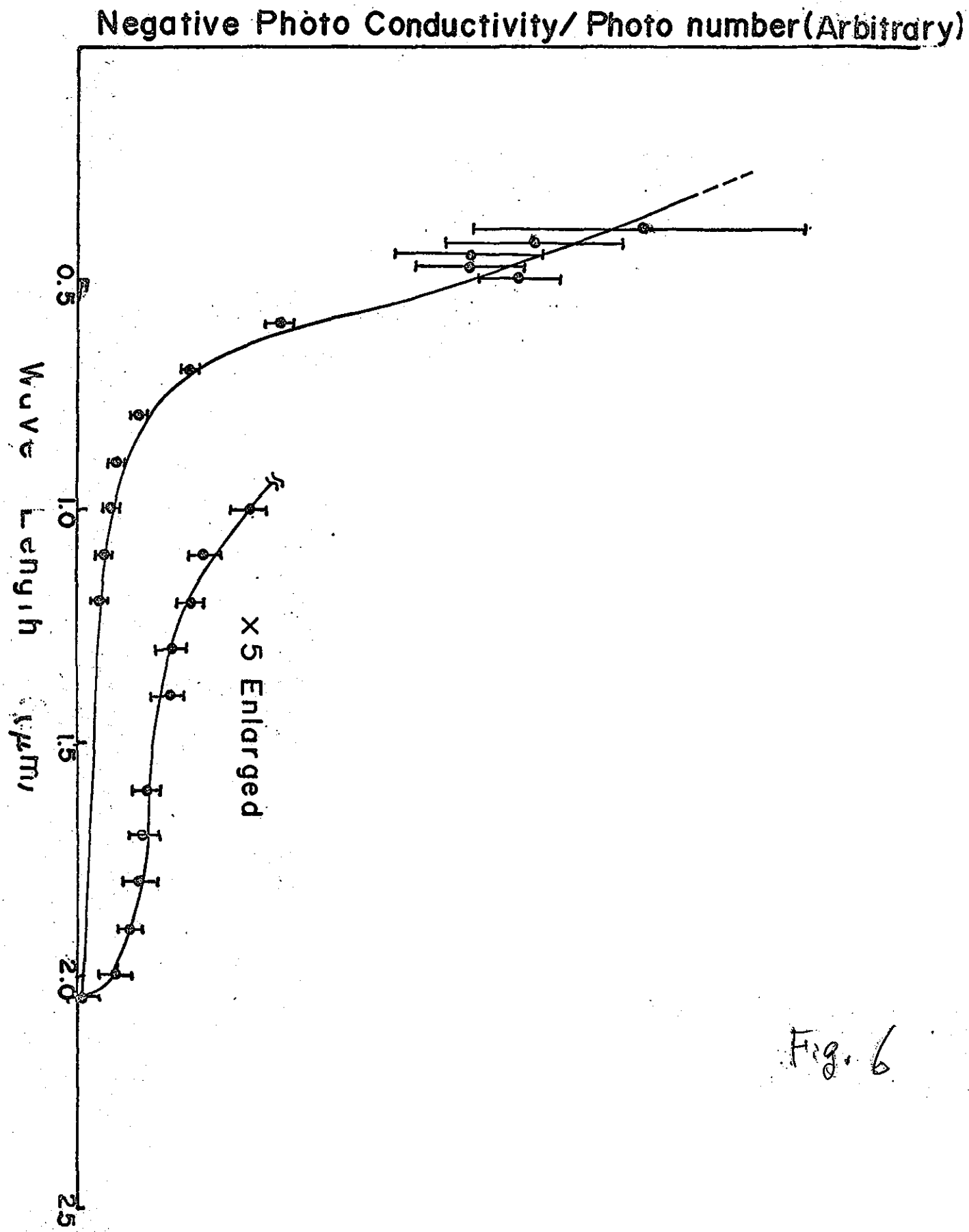
Negative Photo Conductivity/ Photo number(Arbitrary)
Wave Length (μm)
0.5
1.0
1.5
2.0
2.5
X5 Enlarged

Fig. 6

Acknowledgement

I would like to thank Professor M. Date for a number of useful discussions which increased my insight and understanding of this study. I would also like to thank Dr. K. Okuda, Mr. K. Toyokawa, Mr. M. Wake and Mr. O. Ichikawa for their helpful and valuable contributions of this work.